ASYMPTOTICS BEATS MONTE CARLO: THE CASE OF CORRELATED LOCAL VOL BASKETS

CHRISTIAN BAYER AND PETER LAURENCE

To the memory of Peter Laurence, who passed away unexpectedly during the final stage of the preparation of this manuscript.

Abstract. We consider a basket of options with both positive and negative weights, in the case where each asset has a smile, e.g. evolves according to its own local volatility and the driving Brownian motions are correlated. In the case of positive weights, the model has been considered in a previous work by Avellaneda, Boyer-Olson, Busca and Friz [3]. We derive highly accurate analytic formulas for the prices and the implied volatilities of such baskets. The relative errors are of order 10^{-4} (or better) for $T = \frac{1}{2}$, 10^{-3} for $T = 2$, and 10^{-2} for $T = 10$. The computational time required to implement these formulas is under two seconds even in the case of a basket on 100 assets. The combination of accuracy and speed makes these formulas potentially attractive both for calibration and for pricing. In comparison, simulation based techniques are prohibitively slow in achieving a comparable degree of accuracy. Thus the present work opens up a new paradigm in which asymptotics may arguably be used for pricing as well as for calibration.

1. Introduction

1.1. **Setting.** In a multivariate model for the evolution of forward prices of the form,

$$dF_i(t) = \sigma_i(F_i(t))\, dW_i(t),\ i = 1, \dots, n, \tag{1.1a}$$

$$\langle dW_i(t), dW_j(t) \rangle = \rho_{ij} dt, \tag{1.1b}$$

where $\rho_{ij}, i, j = 1, \dots, n$, are constants, consider the problem of pricing a generalized spread option with a payoff of the form

$$P(\mathbf{w}) = \left(\sum_{i=1}^{n} w_i F_i - K \right)^+ ,$$

where the coefficients w_i may be positive or negative (generalized spread options), but where we assume that at least *one* coefficient is positive. (We generally denote by bold face letters like $\mathbf{w}$ or $\mathbf{F}$ vectors of the corresponding scalars $(w_1, \dots, w_n)$ and $(F_1, \dots, F_n)$, respectively.) In this paper we will devote special attention, especially on the implementation side, to the case of a multivariate CEV model, which corresponds to the choice

$$\sigma_i(F_i) = \xi_i F_i^{\beta_i},$$

where β_i and ξ_i are positive constants, the most popular choice among practitioners being to choose $0 < \beta_i \leq 1$, which ensures that $F_i(T)$ are local martingales. However all asymptotic formulas are valid and stated for the full family of models described by (1.1).

P.L. would like to thank Gérard Ben Arous for many interesting and instructive discussions concerning the heat kernel expansion and thanks Gérard and especially Esteban Tabak, for their hospitality at the Courant Institute.

The family of models represented by (1.1) includes a host of models that are very popular in finance. A discussion of the history of this problem and a detailed discussion of our contribution will be given in the following sections. But as a warm-up, let us discuss the use of asymptotics for pricing in such models against the backdrop of a few notable examples. These examples are meant to illustrate two special cases of (1.1), which allow special analytical and numerical pricing methodologies in that they admit closed form solutions.

The case $n = 1$ and $\sigma(F) = \xi F^{\beta}$, is the famous constant elasticity of variance (CEV) model, which is closely related to Bessel processes. The elasticity parameter β controls the steepness of the implied volatility skew. The transition density in such a model admits a closed form solution in terms of Bessel functions [28]

$$p(F_0, F_T, T) = \frac{F_0^{\frac{1}{2}} F_T^{\frac{1}{2}-2\beta}}{\xi^2|\beta-1|T} I_{|\nu|}\left(\frac{F_0^{1-\beta} F_T^{1-\beta}}{\xi^2(1-\beta^2)T}\right) \; e^{-\frac{F_0^{-2(\beta-1)}+F_T^{-2(\beta-1)}}{2\xi^2(1-\beta)^2 T}}$$

where I_ν is the modified Bessel function of the first kind of order ν and where $\nu = \frac{1}{2(\beta-1)}$. Although there is an exact solution in this case, a series expansion thereof converges quite slowly and a more computationally efficient way to calculate a call option price of an implied volatility, even in this one dimensional setting, is arguably to use an asymptotic expansion. Indeed, thanks to the work of Hagan and Woodward [22], practitioners have long preferred to use such asymptotic expansions for calibration. These expansions were extended by Gatheral, Hsu, Laurence, Ouyang and Wang [17], to first order asymptotic expansion of the implied volatility that yields prices with a relative accuracy 10^{-5} in typical volatility environments, for up to 2 years. Since the CEV diffusion has a positive probability of reaching the boundary, this accuracy decreases when the initial point F_0 gets close to the boundary. But for short times to maturity, it was proven rigorously in [17] that the "principle of not feeling the boundary" holds in this case.

A second special case of the family of models considered is the case where n is large (say ≥ 5) and where $\sigma_i(F_i) = \xi_i F_i$. This is the historically important "Black-Scholes" setting, of a (here) multidimensional lognormal distribution. The transition density can be expressed in closed form and basket call option prices can, in principle, be obtained by integrating the basket call option payoff against this lognormal density. So, once more, in this particular case, a closed form solution is well known, but, when the number of assets is large, it is very difficult to take advantage of it in the time frames needed in a trading desk. Indeed all known Monte-Carlo based evaluations of the multidimensional integral are very slow. By contrast, the asymptotic expansions provided in this paper are very accurate and yield a call option price in less than 2 seconds, even in the case of 100 assets. Moreover, when $\beta_i \neq 1$, the situation is further complicated by the absence, to the best of our knowledge, of a closed form representation for the transition densities. Whereas this has no effect on the accuracy or speed of the asymptotic expansions. After these preliminary remarks let us discuss in more detail the various notions of implied volatility that we will make use of in this paper.

The Black-Scholes implied volatility,

$$\sigma_{BS} = IV(F_0, K, T),$$

corresponding to an observed call option price is the value of the volatility σ_{BS} having the property that the Black-Scholes price of an asset with strike K, price F_0, and time to maturity T and volatility σ_{BS} matches the quoted price. In the case of generalized *spread*

options, for which some of the weights can be negative, the basket,

$$\sum_{i=1}^{n} w_i F_i,$$

may have a negative value at time zero or can start out positive and become negative at a later time. On the other hand the spot price in the Black-Scholes setting always remains positive. It does not make much sense to quote an equivalent Black-Scholes price on an asset that is initially, or can at a later time become negative. It seems more natural in such cases to define a *Bachelier* dynamics for the underlying and then to seek a Bachelier, sometimes also called "normal", implied volatility. In any case, as mentioned in the introduction, an asymptotic value of implied volatility, whether Black-Scholes *or* Bachelier, can be viewed in the present context as a tool to determine quickly, efficiently and analytically, the *price* of the generalized spread option. Moreover, once one has determined a Bachelier implied volatility, it is straightforward to determine its Black-Scholes implied volatility equivalent. In fact the latter follows immediately from the results in [17]. Thus in this paper, our approach will be:

- For baskets with positive weights, i.e. index options, we will determine an asymptotic formula for the Black-Scholes implied volatility.
- For baskets in which one or more weights are negative, we will make use of a Bachelier implied volatility, for which we now give a precise definition.

The Bachelier model is a model in which the underlying follows the process

$$\begin{aligned} dF(t) &= F_0 \sigma dW(t), \\ F(0) &= F_0. \end{aligned}$$

It is usually (implicitly) assumed in the literature that F_0 is positive. In that case, the following formula whose properties are discussed in depth in a recent paper by Schachermayer and Teichmann [39], holds

$$C_B(F_0, K, \sigma, T) = (F_0 - K)\Phi(d_{Bach}) + F_0 \sigma \sqrt{T}\phi(d_{Bach}),$$

where $d_{Bach} = \frac{F_0 - K}{\sigma F_0 \sqrt{T}}$, Φ is the cumulative standard normal distribution and ϕ its density. Note that if F_0 is negative, the above formula cannot be correct as it stands, since it would imply a negative call price. In the Bachelier model, even if the asset's price is initially negative it has a positive probability of attaining a positive value and therefore the call price *should* be positive. A simple adjustment of the above pricing formula restores this property. This was pointed out in a earlier note [2], which treats a very special case of the present paper, i.e. the geometric lognormal case for three assets. Since $-W(t)$ has the same distribution as $W(t)$ and is thus still a standard Brownian motion, letting $\widetilde{W}(t) = -W(t)$, we have

$$\begin{aligned} dF(t) &= |F_0| \sigma d\widetilde{W}(t), \\ F(0) &= F_0. \end{aligned}$$

It follows that the formula below is a universally valid version of the Bachelier pricing formula that holds both in the case where F_0 is negative *and* when it is positive:

$$C_B(F_0, K, \sigma, T) = (F_0 - K)\Phi(d_B) + |F_0| \sigma \sqrt{T}\phi(d_{Bach}), \tag{1.2a}$$

$$d_{Bach} = \frac{F_0 - K}{|F_0| \sigma \sqrt{T}}. \tag{1.2b}$$

We will use (1.2) in pricing baskets when one or more of the weights are negative. The exact contributions will be detailed below. But we begin with a literature review to gain a broader perspective and to better put our contribution in context.

1.2. **Literature Review.**

1.2.1. *Lognormal case.* Our treatment contains the very popular lognormal case as a special case, corresponding to the choice $\beta_i = 1, i = 1 \dots n$. As the present work applies both to the case of positive and negative weights, we review some of the contributions of which we are aware, but since the literature is quite vast, we cannot claim to give an exhaustive list.

In the lognormal setting with positive weights there is a significant literature to which various authors have made important contributions. It is difficult to give an exhaustive review. We mention here the papers by Milevski and Posner [30], [31] who use an approximation based on the Gamma function, the paper by Ju [25] who makes use of an asymptotic approach based on the expansion of the characteristic function for small volatilities and a recent paper by Duck and Widdicks [14]. The paper by Carmona and Durlemann provides upper and lower bounds that are quite tight [11].

In the case of one negative weight and $n = 2$, still in the lognormal setting, the case $K = 0$, i.e. the so-called exchange option, has received special attention, as it allows for an exact pricing formula. This is the famous Margrabe formula. In the case $K \neq 0$, still for $n = 2$, Kirk's formula is a favorite among practitioners. This is a very compact formula that provides good accuracy for a formula of its simplicity. Carmona and Durlemann in their review paper [10] also provide approximations for the two asset spread option. Among the various approximations for two-asset spread options, still in the lognormal setting, one stands out from the rest in that it's accuracy is so good that it is "difficult to beat" using Monte-Carlo simulation in the sense that "beating" its accuracy may require millions of paths. This is the formula of Bjerkstund and Stensland [9].

Next, we have multi-asset ($n \geq 3$) spread options in the lognormal setting. In a recent paper Alos, Eydeland and Laurence [2] show that Kirk's formula can be derived from a *decomposition formula* that allows one to view Kirk's approximation as the first in a hierarchy of ever better (but increasingly complicated) approximations. In the multi-asset lognormal setting we also note the recent contributions by Li et al. [27] and by Alexander et al. [1].

1.2.2. *Correlated local volatility processes.* The first contribution dealing with multivariate local volatility pricing models such as (1.1) was, to our knowledge, the paper by Avellaneda, Boyer-Olson, Busca and Friz [3]. This paper is devoted to a family of models that constitutes a special case of the ones considered in the present paper, i.e. to the case of baskets with positive weights, i.e. to index options. The authors provide an approach to determining the zero-th order Black-Scholes implied volatility for this family of models. For this purpose, after determining the geodesics corresponding to the family of models, in order to produce tractable formulas, they introduce a linearization procedure, that provides approximations to the zero-th order implied volatility[1] and corresponding price, when the basket is "close to the money". To determine the sought for implied volatility, the authors first determine the local volatility function for the index itself and then apply the well-known half-slope rule.

[1]The first in a hierarchy of approximations of the form $\sigma_{BS} = \sigma_0^{BS} + \sum_{i=1}^{N} \sigma_i^{BS} T^i, N \geq 1$, as explained in the body of the present paper.

This leads to nice, compact formulas for the implied volatility. The zero-th order formula of Avellaneda, Boyer-Olson, Busca, and Friz depends on an approximation of the point of minimum distance from the initial point to a hyperplane, the so-called "optimal" (or minimizing) configuration. As mentioned above, the authors linearization procedure fares quite well only "close to the money", i.e., when

$$\left|\sum_{i=1}^{n} w_i F_i(0) - K\right|$$

is sufficiently small. In addition to providing, in the correlated and uncorrelated CEV case, a quick, simple and efficient way to determining the *true* minimizer in all regimes including far from the money, in this paper we go further to derive a *first order correction* σ_1. It is this new first order correction that allows us achieve a surprising level of accuracy, as we will see in the numerical experiments.

Another contribution in the direction of asymptotics for baskets with positive weights appears in the book of Henry-Labordère [23]. As we will do here, Henry-Labordère makes use of a heat kernel expansion. He also provides a first order correction to the zero-th order implied volatility, which is however quite different from ours, and is not optimal, since it makes use of a formula for the implied volatility in one factor local volatility models which is not the optimal one, as given in [17]. Also Henry-Labordère does not discuss the crucial issue of efficiently and accurately determining the minimizing configuration and does not discuss baskets with negative weights. The approach by Piterbarg [37], using Markovian projection, yields a fairly good approximation in the multi-asset local volatility setting, by replacing conditional expectations with Gaussian approximations thereof. Lastly, Takahashi et al. have very recently extended their powerful asymptotic approximation techniques using Malliavin calculus to the basket option pricing setting, [40]. They consider multi-asset Sabr models, of which our multi-dimensional local volatility model is a special case (corresponding to zero vol of vol). A comparison of the accuracy of our results with those of Takahashi is in progress. However as described below, our approximations are *highly* accurate.

Although this paper is written in the spirit of classical asymptotics, i.e., with the objective of providing expansions that are useful, quick and accurate, we show in Section 4, thanks to the work by Varadhan [41], Azencott [5] and Ben Arous [7], the theory required to fully justify these expansions and provide error bounds already exists, under certain not too stringent technical conditions, even in the setting of degenerate diffusions and we sketch how to put this theory to work in our context.

1.3. **Our contribution.** In this paper we will show that the exact (ie., highly accurate) value of the minimizing configuration, and the corresponding minimal *value*, can be easily determined. This improved approximation of the zero-th order price often captures more than $95-99\%$ of the actual price. To this zero-th order approximation we add a first order one, which leads to additional significant improvements in the accuracy. The accuracy of the resulting approximations is, in some cases, so good that it leads us to coin the phrase "asymptotics beats Monte-Carlo". Indeed, in many cases more than 99.9% of the price is captured by its first order approximation. This seems to open the way for a *new role* for such asymptotics. In the past the main role of asymptotic results has arguably been as a calibration rather than as a pricing tool. A case in point, the ground breaking asymptotic results of Hagan et al. [21], and Henry-Labordère [23], for the implied volatility in the SABR model have been used by practitioners primarily as a method to *calibrate* the implied volatility surface, rather than as a means to *price* an option. For accurate pricing

of an option in a local volatility setting, practitioners tend to use finite difference methods or sophisticated higher order stochastic numerical methods such as Ninomiya-Victoir [35] or innovative multi-level techniques introduced by Giles [19]. But in the context of baskets with a large number of assets and state dependent driving diffusions, Monte-Carlo methods are extremely slow and the trade-off between speed and accuracy rapidly becomes quite poor as the number of assets increases, even more so when finite difference methods are used. In this context, since the asymptotics produces prices with high accuracy, almost instantaneously, it can be argued that asymptotic formulas for the prices can also be viewed as a *pricing* and *hedging* tool. The application of the present techniques to calculate the greeks is straightforward but lengthy and will be presented elsewhere. In our numerical results, we focus on the special case in which the local volatilities are powers of the underlying assets, i.e., CEV processes. All our main asymptotic formulas (2.19) and (2.17) as well as the ingredients needed to calculate these are available in closed form for *any* prescription of the local volatilities – possibly up to one-dimensional line-integrals, which can be easily calculated numerically.

1.4. **Basket Carr-Jarrow formula.** Consider a basket option with payoff $\mathcal{B} = \sum w_i F_i$ and weights $w_i \in \mathbf{R}$. Take the Itô derivative of the basket's price:

$$\begin{aligned} d\sum_{i=1}^n w_i F_i(t) &= \sum_{i=1}^n w_i \sigma_i(F_i(t)) dW_i(t) \\ &= \sqrt{\underbrace{\sum_{i,j=1}^n w_i w_j \sigma_i(F_i(t)\sigma_j(F_j(t))\rho_{ij}}_{\sigma^2_{\mathcal{N},\mathcal{B}}}}\, d\overline{W}(t), \end{aligned}$$

for a new Brownian motion $\overline{W}$. Here we have used the notation $\sigma_{\mathcal{N},\mathcal{B}}$ to indicate the "normal volatility" of the basket which must not be confused with the lognormal (Black) volatility $\sigma_{\mathcal{B}} = \frac{\sigma_{\mathcal{N},\mathcal{B}}}{\sum_{i=1}^n w_i F_i}$ used in reference [3]. Therefore, by the Itô-Tanaka formula we have

$$d\left(\sum_{i=1}^n w_i F_i(t) - K\right)^+ = \sum_{i=1}^n w_i \mathbf{1}_{\sum w_i F_i(t) > K}\, dF_i(t) + \frac{1}{2}\delta_{\{\mathbf{F}(t):\sum w_i F_i(t) = K\}}\, \sigma^2_{\mathcal{N},\mathcal{B}}(\mathbf{F}(t))dt.$$

Integrating we obtain

$$\begin{aligned} \left(\sum_{i=1}^n w_i F_i(T) - K\right)^+ &= \left(\sum_{i=1}^n w_i F_i(0) - K\right)^+ + \\ &+ \sum_{i=1}^n w_i \int_0^T \mathbf{1}_{\sum w_i F_i(u) > K}\, dF_i(u) + \frac{1}{2}\int_0^T \delta_{\{\mathbf{F}(u):\sum w_i F_i(u) = K\}}\, \sigma^2_{\mathcal{N},\mathcal{B}}(\mathbf{F}(u))du. \end{aligned}$$

Letting $\mathcal{E}_K = \{\mathbf{F} \in \mathbf{R}^n_+ : \sum w_i F_i = K\}$ and taking conditional expectations with respect to the filtration $\mathcal{F}_t$ at time t, we obtain, assuming $F_i(t)$ is a martingale for each i[2]:

$$C_{\mathcal{B}}(\mathbf{F}_t, K, T) = \left(\sum_{i=1}^n w_i F_i(t) - K\right)^+ + \frac{1}{2}\int_t^T E\left[\sigma^2_{\mathcal{N},\mathcal{B}}\, \delta_{\mathcal{E}(K)}(\mathcal{B}_t)\,|\,\mathcal{F}_t\right] dt.$$

[2] In many cases of interest, $F_i(t)$ is only a local martingale and not a martingale. But the discrepancy is not "felt" for short times, since the set of paths that can reach the boundary have small probability, in this limit. This is known as the principle of "not feeling the boundary" for small times and is born out by our numerical results. More surprisingly the boundary is not felt, even for quite large times.

Letting $|w| = \sqrt{\sum_{i=1}^{n} w_i^2}$, and denoting by H_{n-1} the Hausdorff measure, which on the hyperplane $\mathcal{E}_K$ coincides with the Lebesgue measure, a simple use of the co-area formula (see [15]), and using that $\left|\nabla(\sum_{i=1}^{n} w_i F_i)\right| = |w|$, we see that the expectation, when expressed in terms of the joint transition density, is given by:

$$C_{\mathcal{B}}(\mathbf{F}_0, \mathbf{K}, T) = \left(\sum_{i=1}^{n} w_i F_i(0) - K\right)^+ + \frac{1}{2}\int_0^T \frac{1}{|w|} \int_{\mathcal{E}(K)} \sigma^2_{N,\mathcal{B}}(\mathbf{F}) p(\mathbf{F}_0, \mathbf{F}, u) dH_{n-1}(\mathbf{F}) du.$$

Therefore, we arrive at the proposition:

Proposition 1.1. *The value of a call option on a basket $\mathcal{B}$ is given by*

$$C_{\mathcal{B}}(\mathbf{F}_0, K, T) = \left(\sum_{i=1}^{n} w_i F_i(0) - K\right)^+ + \\ + \frac{1}{2}\int_0^T \frac{1}{|w|} \int_{\mathcal{E}(K)} \sum_{i,j=1}^{n} w_i w_j \sigma_i(F_i)\sigma_j(F_j)\rho_{ij} p(\mathbf{F}_0, \mathbf{F}, u) dH_{n-1}(\mathbf{F}) du. \tag{1.3}$$

2. A general asymptotic expansion procedure

The starting point is the basket Carr-Jarrow formula derived above. The key step in the approach is to plug into this formula a good approximation for the transition density, for small, dimensionless times to maturity (i.e., a typical volatility times the square root of the time to maturity). The approximation technique we use in this paper is the heat kernel expansion, whose main features we recall in the appendix. The heat kernel expansion is an expansion with an exponential, Gaussian looking term, that multiples a series in ascending integral powers of time to maturity.

We will see that to derive a first order expansion for the implied volatility for a basket option, i.e., an expansion of the form

$$\sigma_{\mathrm{BS}}(K, T) = \sigma_{\mathrm{BS},0} + T\sigma_{\mathrm{BS},1},$$

it will only be necessary to use a heat kernel expansion up to the zero-th order,

$$p(\mathbf{F}_0, \mathbf{F}, T) \simeq \frac{\sqrt{g(\mathbf{F})}}{(2\pi T)^{\frac{n}{2}}} e^{-\frac{d^2(\mathbf{F}_0, \mathbf{F})}{2T}} u_0(\mathbf{F}_0, \mathbf{F}), \tag{2.1}$$

where we denote by $\sqrt{g}$ the square root of the determinant of the Riemannian metric associated to the diffusion whose entries are $g^{ij} = \{\sigma_i(F_i)\sigma_j(F_j)\rho_{ij}\}_{i,j=1}^n$. Recall that the metric's components are g_{ij} where $\{g_{ij}\}$ is the inverse of $\{g^{ij}\}$. Also, in (2.1), the term d in the exponent of the exponential is the Riemannian distance in the metric g. In all local volatility models with constant correlations, it is easy to see by simple changes of variables that the Riemannian distance is given by

$$d^2(\mathbf{F}_0, \mathbf{F}) = \sum_{i,j=1}^{n} q_i \Lambda_{i,j} q_j, \tag{2.2}$$

where

$$q_i := \int_{F_{0,i}}^{F_i} \frac{1}{\sigma_i(u)} du$$

and where Λ is inverse of the correlation matrix. In case the integral above diverges, one can use a different lower limit of integration. To conclude our discussion of the ingredients in (2.1), u_0 is the zero-th order *heat kernel coefficient*. As explained in the appendix, for the class of local volatility models with constant correlations, that we explore in this paper, u_0 can be given in *closed form*.

After this preliminary discussion, we can begin our derivation of the asymptotics. In the rest of this section the *specific form* of the metric g, local volatility functions $\sigma_i, i = 1, \dots, n$, and Riemannian distance function d and zero-order heat kernel coefficient u_0 does not come into play. This means that most of this section, in particular the final formula (2.12), derived here, would still apply (with certain simple adjustments) for a more general class of local volatility models, such as the models with *non-constant* correlations.

Recalling the notation $\sigma^2_{N,\mathcal{B}}(\mathbf{F}) = w_i w_j \sigma_i(F_i)\sigma_j(F_j)\rho_{ij}$, and also denoting

$$\alpha_0 \coloneqq \sqrt{g}(\mathbf{F})\sigma^2_{N,\mathcal{B}}(\mathbf{F}) \tag{2.3}$$

$$C \coloneqq -\log(\alpha_0(\mathbf{F})u_0(\mathbf{F}_0, \mathbf{F})), \tag{2.4}$$

we may re-write the integral appearing in (1.3) in the form

$$\begin{aligned}\int_0^T \frac{1}{|w|} \int\limits_{\mathbf{F}\in\mathcal{E}(K)\cap\mathbf{R}^n_+} \sum_{i,j=1}^n w_i w_j \sigma_i(F_i)\sigma_j(F_j)\rho_{ij}\, p(\mathbf{F}_0, \mathbf{F}, t) dH_{n-1} dt \\ \cong \int_0^T \frac{dt}{(2\pi t)^{\frac{n}{2}}} \frac{1}{|w|} \int\limits_{\mathbf{F}\in\mathcal{E}(K)\cap\mathbf{R}^n_+} e^{-\frac{d^2(\mathbf{F}_0,\mathbf{F})}{2t} - C(\mathbf{F}_0,\mathbf{F})} dH_{n-1},\end{aligned} \tag{2.5}$$

where we have approximated the heat kernel by its zero-th order approximation. The first step is to transform the integral on the $n-1$ dimensional subspace $\mathcal{E}_K$ of $\mathbf{R}^n$ into an integral over $\mathbf{R}^{n-1}$, by eliminating one of the variables, say the n-th one, using the relation

$$F_n(F_1, \dots, F_{n-1}, K) = \frac{1}{w_n}\left(K - \sum_{i=1}^{n-1} w_i F_i\right). \tag{2.6}$$

Let us denote

$$\begin{aligned}\mathbf{G} &\coloneqq (F_1, \dots, F_{n-1}) \in \mathbf{R}^{n-1}_+, \\ \mathcal{G}_K &\coloneqq \left\{\mathbf{G} \in \mathbf{R}^{n-1} \;\middle|\; \sum_{i=1}^{n-1} w_i F_i < K\right\},\end{aligned}$$

so that for our hyperplane's intersection

$$\mathcal{E}_K \cap \mathbf{R}^n_+ = \left\{\mathbf{F} \in \mathbf{R}^n_+ \;\middle|\; \mathbf{F} = \left(\mathbf{G}, \frac{1}{w_n}\left(K - \sum_{i=1}^{n-1} w_i F_i\right)\right), \mathbf{G} \in \mathcal{G}_K\right\}.$$

Note that the set $\mathcal{G}_K$ is introduced in order to ensure that F_n in (2.6) is non-negative, as it needs to be. The set $\mathcal{E}_K$ is an $n-1$ dimensional hyperplane in $\mathbf{R}^n_+$.

Consider now the inner integral. Note that, when we parametrize the hyperplane $\mathcal{E}_K$ using $(F_1, \dots, F_{n-1})$, as in (2.6)

$$F_K(F_1, \dots, F_{n-1}) = (F_1, \dots, F_{n-1}, F_n(F_1, \dots, F_{n-1}, K)),$$

we will assume that the weight multiplying F_n is *positive*. This can always be achieved by choosing as the n-th asset one of the assets with a positive weight. Then for the surface

measure, we have

$$dH_{n-1} = \sqrt{1+|\nabla F_n|^2}dF_1\dots dF_{n-1} = \frac{|w|}{|w_n|}dF_1\dots dF_{n-1}.$$

In this notation, the inner integral reads

$$\frac{|w|}{|w_n|}\int_{\mathbf{G}_K} e^{-\frac{d^2(\mathbf{F}_0,\mathbf{F}_K)}{2t}-C(\mathbf{F}_0,\mathbf{F}_K)}dF_1\dots dF_{n-1}.$$

We now approximate the value of this integral using standard *Laplace asymptotics* for multiple integrals. Under certain conditions, whose validity in the present setting is discussed in Section 4, and which in all the examples considered in this paper were indeed verified by the numerical results, we may approximate the value of the above integral by a series in inverse powers of T, with coefficients determined by the behavior of the integrand close to the point where the exponent d^2 reaches its minimizing value. In particular, assuming that the distance function d has, for each initial point $\mathbf{F}_0$, only one point realizing the minimum of d^2 on $\mathcal{G}_K$, and assuming that this minimum is achieved in the *interior* of $\mathcal{G}_K$, denoting this minimum point by $\mathbf{G}^*$, and

$$\begin{aligned}\mathbf{G}^* &= \text{argmin}_{\mathbf{G}\in\mathbf{G}_K} d^2(\mathbf{F}_0,(\mathbf{G},F_n(\mathbf{G},K)),\\ &= d^2(\mathbf{F}_0,\mathcal{E}_K).\end{aligned} \tag{2.7}$$

Setting also $\mathbf{F}_K^* = (\mathbf{G}^*, F_n(\mathbf{G}^*,K))$, we see that the integral can be approximated by

$$t^{\frac{n-1}{2}}e^{-\frac{d^2(\mathbf{F}_0,\mathbf{F}_K^*)}{2t}-C(\mathbf{F}_0,\mathbf{F}_K^*)}\times\int_{\mathbf{R}^{n-1}}e^{-\frac{z'Qz}{2}}dz_1\dots dz_{n-1} = t^{\frac{n-1}{2}}e^{-\frac{-d^2(\mathbf{F}_0,\mathbf{F}_K^*)}{2t}-C(\mathbf{F}_0,\mathbf{F}_K^*)}\frac{(2\pi)^{\frac{n-1}{2}}}{|Q|^{\frac{1}{2}}}, \tag{2.8}$$

with

$$Q := D^2\Phi(\mathbf{G}^*),\quad \Phi(\mathbf{G}) := \frac{1}{2}d(\mathbf{F}_0,(\mathbf{G},F_n(\mathbf{G},K)), \tag{2.9}$$

where $D^2\Phi$ denotes the hessian matrix of Φ and $|Q|$ the determinant of Q (assumed different from zero), and $\mathbf{z} := \frac{\mathbf{G}^*-(F_{0,1},\dots,F_{0,n-1})}{\sqrt{t}}$. Thus, bringing back the missing factor, the integrand of (2.5) can therefore be approximated by

$$\frac{1}{|w_n|\sqrt{2\pi t}}e^{-\frac{-d^2(\mathbf{F}_0,\mathbf{F}_K^*)}{2t}-C(\mathbf{F}_0,\mathbf{F_K})}|Q|^{-\frac{1}{2}},$$

which, if we let

$$\hat{C} := C+\frac{1}{2}\log(|Q|), \tag{2.10}$$

can be written as

$$\frac{1}{|w_n|\sqrt{2\pi t}}e^{-\frac{-d^2(\mathbf{F}_0,\mathbf{F}_K^*)}{2t}-\hat{C}(\mathbf{F}_0,\mathbf{F}_K^*)}.$$

Now, integrating this result with respect to t, for t between 0 and T, we obtain:

$$\frac{1}{\sqrt{2\pi}|w_n|}\int_0^T\frac{1}{\sqrt{t}}e^{\frac{-d^2(\mathbf{F}_0,\mathbf{F}_K^*)}{2t}-\hat{C}(\mathbf{F}_0,\mathbf{F}_K^*)}dt = \frac{1}{\sqrt{2\pi}|w_n|}e^{-\hat{C}(\mathbf{F}_0,\mathbf{F}_K^*)}\int_0^T\frac{1}{\sqrt{t}}e^{\frac{-d^2(\mathbf{F}_0,\mathcal{E}_K)}{2t}}dt. \tag{2.11}$$

The asymptotics of the integral in (2.11) has already been determined in several places (eg.,Henry-Labordère [23] and [17]) (see bottom of page 16), and to leading order it gives

$$\frac{1}{|w_n|}\int_0^T\frac{e^{-\frac{d_*^2}{2t}}}{\sqrt{t}}dt\sim\frac{2}{d_*^2}e^{-\frac{-d^2(\mathbf{F}_0,\mathbf{F}_K^*)}{2T}}T^{\frac{3}{2}},\quad T\to 0, \tag{2.12}$$

where $d_* = d(\mathbf{F}_0, \mathbf{F}_K^*)$. So that plugging (2.12) into (2.11), we get for (2.5) the approximation

$$\frac{1}{|w_n|\sqrt{2\pi d_*^2}} e^{-\hat{C}(\mathbf{F}_0,\mathbf{F}_K^*)} e^{-\frac{-d^2(\mathbf{F}_0,\mathbf{F}_K^*)}{2T}} T^{\frac{3}{2}}.$$

Note that we do *not* express the factor d_*^2 via a (new) exponential expression for reasons that will be clear later on, during the matching phase. Thus

Proposition 2.1. *The expansion of the call prices in drift-less local volatility models is asymptotically equivalent to*

$$C_{\mathcal{B}}(\mathbf{F}_0, K, T) = \left(\sum_{i=1}^n w_i F_i(0) - K\right)^+ + \frac{1}{2\sqrt{2\pi}|w_n| d_*^2} e^{-\hat{C}(\mathbf{F}_0,\mathbf{F}_K^*)} e^{-\frac{-d^2(\mathbf{F}_0,\mathbf{F}_K^*)}{2T}} T^{\frac{3}{2}} \tag{2.13}$$

as $T \to 0$, where $\mathbf{F}_K^*$, is the point on the hyperplane $\sum_{i=1}^n w_i F_i = K$, at minimum (Riemannian) distance from the initial point $\mathbf{F}_0$ and where $\hat{C}$ is defined by (2.10).

2.1. **Matching to Bachelier model when one or more of the weights is negative.** Recall that Bachelier's model is described by

$$dF(t) = \sigma_B |F_0| \, dW(t), \quad F(0) = F_0 \in \mathbf{R}, \ 0 \le t \le T.$$

In this case, assuming zero interest rates, the Bachelier price of a call option was given in (1.2).

From the results in [17], applied to the case where the local volatility σ_L is given by $\sigma_B|F_0|$, the *difference* between the call price and its intrinsic value is given, to order $T^{3/2}$ by

$$\frac{1}{\sqrt{2\pi}} e^{-d_B(F_0,K)^2/2T} \frac{1}{d_B(F_0,K)^2} \sigma_L(K,t) u_0(F_0,K,t) T^{3/2}, \tag{2.14}$$

where the one dimensional signed distance function is given by

$$d(F,K) = \int_K^{F_0} \frac{1}{\sigma_L(u)} du,$$

which, in the Bachelier case, becomes

$$d_B(F_0,K) = \frac{F_0 - K}{\sigma_B |F_0|}.$$

Also, the one dimensional heat kernel coefficient u_0 is in the time homogeneous case given simply by

$$u_0^{(1d)}(F,K,t) = \sqrt{\frac{\sigma_L(F,t)}{\sigma_L(K,t)}},$$

which is identically equal to 1 in the Bachelier case. Therefore, keeping terms up to order $T^{3/2}$ we have for the difference between the call price and its intrinsic value,

$$\frac{1}{2\sqrt{2\pi d_B^2}} e^{-\frac{(F_0-K)^2}{2\sigma_B^2 F_0^2 T}} \sigma_B |F_0| T^{3/2}.$$

Now we try to determine the coefficients in the expansion of

$$\sigma_B = \sigma_{B,0} + \sigma_{B,1} T + O(T^2).$$

Since we are assuming a Bachelier dependence for the *basket*, we let

$$\overline{F}_0 = \sum_{i=1}^{n} w_i F_{0,i}.$$

We set the Bachelier price equal to the basket option price and cancel like terms to get

$$\frac{1}{d_B^2} e^{-\frac{(\overline{F}_0-K)^2}{\sigma_B^2 \overline{F}_0^2 T}} \sigma_B |\overline{F}_0| = \frac{1}{d_*^2} e^{-\frac{\Phi}{T} - \hat{C} - \log(|w_n|)}.$$

Denoting by $d_{B,0}$ the corresponding expansion of d_B, the expansion of the exponent on the left hand side up to zero-th order yields

$$\frac{1}{d_{B,0}^2} e^{-\frac{(\overline{F}_0-K)^2}{2\sigma_{B,0}^2 \overline{F}_0^2 T}} e^{\frac{(\overline{F}_0-K)^2 \sigma_{B,1}}{\overline{F}_0^2 \sigma_{B,0}^3} + \log(|\overline{F}_0|\sigma_{B,0})}.$$

Matching the exponential terms we get

$$d_{B,0}^2 = \frac{(\overline{F}_0 - K)^2}{\sigma_{B,0}^2 \overline{F}_0^2} = d_*^2, \tag{2.15}$$

or equivalently

$$\sigma_{B,0} = \frac{|\overline{F}_0 - K|}{d_* |\overline{F}_0|}. \tag{2.16}$$

Using (2.15) and equating the terms of order zero in the exponent, we find

$$\hat{C} = -\left(\frac{(\overline{F}_0 - K)^2 \sigma_{B,1}}{\overline{F}_0^2 \sigma_{B,0}^3} + \log(|w_n|\sigma_{B,0}|\overline{F}_0|) \right),$$

so that we get:

Proposition 2.2. *The first order normal (Bachelier) implied volatility, for a basket option on n assets evolving according to the dynamics (1.1), is given by*

$$\sigma_{B,1} = -\frac{\overline{F}_0^2 \sigma_{B,0}^3}{(\overline{F}_0 - K)^2} \left(\hat{C} + \log(\sigma_{B,0}|\overline{F}_0||w_n|) \right) \tag{2.17}$$

where $\overline{F}_0$ is the initial value of the basket, $\sigma_{B,0}$ is given by (2.16), and $\hat{C}$ is defined by (2.10).

2.2. **Matching to Black-Scholes in positive weights case.** As demonstrated in Gatheral et.al. [17], setting $\xi = \log\left(\frac{F_0}{K}\right)$ the asymptotics of the Black-Scholes call prices is given up to order $T^{\frac{3}{2}}$ by

$$\frac{\sqrt{F_0 K}}{\sqrt{2\pi}} e^{-\frac{\xi^2}{2\sigma_{\mathrm{BS},0}^2 T}} \frac{\sigma_{\mathrm{BS}}^3 T^{\frac{3}{2}}}{\xi^2} = \frac{\sqrt{F_0 K}}{\sqrt{2\pi}} \frac{1}{d_{BS}^2} e^{-\frac{\xi^2}{2\sigma_{\mathrm{BS},0}^2 T}} \sigma_{BS},$$

which we hereby apply with $F_0 = \overline{F}_0$. Expanding again, up to the first order

$$\sigma_{\mathrm{BS}} \sim \sigma_{\mathrm{BS},0} + T\sigma_{\mathrm{BS},1}, \quad T \to 0,$$

and canceling the term $\frac{1}{\sqrt{2\pi}} T^{\frac{3}{2}}$, we have

$$e^{-\frac{\xi^2}{2T\sigma_{\mathrm{BS},0}^2} + \frac{\xi^2 \sigma_{\mathrm{BS},1}}{\sigma_{BS,0}^3}} \sqrt{\overline{F}_0 K} \sigma_{BS,0}.$$

Matching the exponential terms gives

$$\sigma_{\mathrm{BS},0} = \frac{|\xi|}{d}. \tag{2.18}$$

At the zero-th order we get

$$e^{-\hat{C}-\log(|w_n|)} = e^{\frac{\xi^2\sigma_{\mathrm{BS},1}}{\sigma^3_{BS,0}}}\sqrt{\overline{F}_0 K}\sigma_{BS,0},$$

so that we have the following

Proposition 2.3. *The first order Black-Scholes implied volatility, for a basket option, with all positive, weights on n assets, evolving according to the dynamics (1.1) is given by*

$$\sigma_{\mathrm{BS},1} = -\frac{\sigma^3_{\mathrm{BS},0}}{\xi^2}\left(\hat{C} + \log\left(\sigma_{BS,0}|w_n|\sqrt{\overline{F}_0 K}\right)\right). \tag{2.19}$$

where $\overline{F}_0$ is the initial value of the basket, $\sigma_{\mathrm{BS},0}$ is given by (2.18), and where $\hat{C}$ is defined by (2.10).

3. Determining the minimum value

The key step in applying the method in this paper is to calculate accurately and quickly the minimum value of the squared distance function of a point to a hyperplane. It turns out that this can be done with a device as simple as multidimensional Newton's iteration. Of course in the presence of local minimizers, it is possible that Newton's method does not converge. Thus, it is necessary to start Newton's iteration with a good initial guess. In seeking good initial points we are concerned with:

- Identifying the only ansatz known heretofore for such a minimizer and for the corresponding minimum, in the (special) *positive weight* case, due to Avellaneda, Boyer-Olson, Busca and Friz, as a linearization of the optimization problem in log moneyness coordinates.
- Providing alternative linearizations which are found to be at least as accurate.
- Deriving a family of higher order, i.e., quadratic approximations to the minimizing configuration.

Concerning the first point, note that the Avellaneda, Boyer-Olson, Busca, Friz [3] formulate the problem of determining the distance of a point to the hyperplane $\mathcal{E}_K$ in terms of the underlying geodesics, rather than directly in terms of the distance function as we do here. Although the approach using geodesics is equivalent to ours, this equivalence is at first sight not all transparent when comparing their nonlinear system to ours. It turns out, however, that if one uses an appropriate linearization of the problem, re-formulated as here (more simply we think) *directly* in terms of the distance function, one easily recovers their approximation for the minimizing configuration. We review their ansatz in the next section and rederive it in our framework in Section 3.3 .

3.1. The approximation due to Avellaneda et al.

Avellaneda et al. in [3] find the following approximation for the optimal configuration. We translate it into our notation. Denote by $\mathbf{F}^*$ the (sought for) optimizing configuration. It is important to note that the local volatility problem in the above authors' approach is denoted

$$dF_i(t) = \sigma_i(F_i(t))F_i(t)dW_i(t)$$

whereas, in our notation, we use $dF_i(t) = \sigma_i(F_i(t))dW_t$. Let

$$x_i^* \coloneqq \log\left(\frac{F_i^*}{F_{0,i}}\right),$$
$$B_0 \coloneqq \sum_{i=1}^n w_i F_{0,i},$$
$$\sigma_B(0)^2 \coloneqq \frac{1}{B_0^2}\sum \sigma_i(F_{0,i})\sigma_j(F_{0,j})F_{0,i}F_{0,j}\rho_{ij}w_i w_j,$$

where, for instance, in the CEV case in their notation, we have

$$\sigma_i(F_i) = \xi_i F_i^{\beta_i - 1},$$

and define

$$p_j = w_i \frac{F_{0,i}}{B_0}.$$

Let $\mathbf{x}^* = (x_1^*, \ldots, x_n^*)$, then

$$x_i* = \frac{\log(\frac{K}{B_0})}{\sigma_B^2(0)} \sum_{j=1}^n \rho_{ij}\sigma_i(F_{0,i})\sigma_j(F_{0,j})p_j. \tag{3.1}$$

3.2. **A linearization in the q variables.** We introduce the q_i-s as the fundamental independent variables. Forward prices F_i are expressed in terms of these. Here

$$q_i(F_i) = \int_{F_{0,i}}^{F_i} \frac{1}{\sigma_i(u)}du.$$

For the sake of concreteness, we are only treating the CEV case in the following. In that case we abuse notation by setting

$$q_i(F_i) \coloneqq \int_{F_{0,i}}^{F_i} \frac{1}{u^{\beta_i}}du = \frac{1}{1-\beta_i}(F_i^{1-\beta_i} - F_{0,i}^{1-\beta_i}).$$

Setting $\mathbf{q} = (q_1, \ldots, q_n)$ and letting $\Lambda = \Sigma^{-1}$ be the inverse of the variance-covariance matrix with entries $\Sigma_{i,j} = \xi_i\xi_j\rho_{i,j}$, $1 \le i, j \le n$, and noting that $d^2(\mathbf{F}_0, \mathbf{F}) = \mathbf{q}^t\Lambda\mathbf{q}$, the minimization problem in these variables reads

$$\min \mathbf{q}^t\Lambda\mathbf{q} : \sum_{i=1}^n w_i F_i(q_i) = K.$$

Since

$$\frac{\partial d^2}{\partial \mathbf{q}} = 2\Lambda\mathbf{q},$$

the constrained problem with Lagrange multiplier λ, using that

$$F_i(q_i) = \left(F_{0,i}^{1-\beta_i} + (1-\beta_i)q_i\right)^{\frac{1}{1-\beta_i}} = F_{0,i} + F_{0,i}^{\beta_i}q_i + \frac{1}{2}\beta_i F_{0,i}^{2\beta_i-1}q_i^2 + O(q_i^3),$$

then gives rise to the condition

$$\begin{aligned}(\Lambda\mathbf{q})_i &= \frac{1}{2}\lambda w_i \frac{\partial F_i}{\partial q_i} \\ &= \frac{1}{2}\lambda w_i\left(F_{0,i}^{\beta_i} + \beta_i F_{0,i}^{2\beta_i-1}q_i\right) + O(q_i^2)\end{aligned} \tag{3.2}$$

The constraint can be expressed as

$$\sum w_i \cdot \left(F_0^i + F_0^{\beta_i} q_i + \frac{1}{2}\beta_i F_{0,i}^{2\beta_i - 1} q_i^2 \right) = K + O\left(|\mathbf{q}|^3\right). \tag{3.3}$$

To lowest order we drop the term multiplying q on the RHS of (3.2) and obtain, letting $(\widetilde{\mathbf{F}}_0)_i = w_i F_{0,i}^{\beta_i}$,

$$\mathbf{q} = \frac{1}{2}\lambda \Lambda^{-1} \widetilde{\mathbf{F}}_0. \tag{3.4}$$

We then apply a linearized version of the constraint $\sum w_i F_i(q_i) = K$, i.e.,

$$\sum w_i (F_{0,i} + F_{0,i}^{\beta_i} q_i) = K$$

or

$$\sum w_i F_{0,i}^{\beta_i} q_i = K - B_0. \tag{3.5}$$

Now multiplying both sides of (3.4) by $\widetilde{\mathbf{F}}_0^t$ and solving for λ we find

$$\lambda = \frac{2(K - B_0)}{\widetilde{\mathbf{F}}_0^t \Lambda^{-1} \widetilde{\mathbf{F}}_0}. \tag{3.6}$$

Inserting this into (3.4) gives

$$\mathbf{q} = \left(\frac{(K - B_0)}{\widetilde{\mathbf{F}}_0^t \Lambda^{-1} \widetilde{\mathbf{F}}_0} \right) \Lambda^{-1} \widetilde{\mathbf{F}}_0. \tag{3.7}$$

Once $\mathbf{q}$ is known, we can use the exact relation $F_i(q_i) = \left(F_{0,i}^{1-\beta_i} + (1-\beta_i) q_i \right)^{\frac{1}{1-\beta_i}}$ to determine $\mathbf{F}$ or alternatively one can use the Taylor expansion thereof.

3.3. **New derivation of the formulas of Avellaneda et al.** In this section we show how to recover the Avellaneda et. al. approximation introduced in Subsection 3.1 in the present framework. Thus we use $x_i = \log\left(\frac{F_i}{F_{0,i}}\right)$ and $X = \log\left(\frac{K}{B_0}\right)$ as the main variables, so that $F_i = F_{0,i} e^{x_i}$. From the relation

$$\sum_{i=1}^n w_i F_i = K,$$

which can be written

$$\sum_{i=1}^n w_i F_{0,i} e^{x_i} = K = B_0 e^{\log\left(\frac{K}{B_0}\right)},$$

we obtain the approximate relation

$$\sum_{i=1}^n w_i F_{0,i}(1 + x_i) = B_0 e^X = B_0(1 + X).$$

So the linearized constraint can be written

$$\sum_{i=1}^n w_i \frac{F_{0,i}}{B_0} x_i = X.$$

Since

$$x_i = \frac{1}{1-\beta_i} \log\left(1 + (1-\beta_i) \frac{q_i}{F_{0,i}^{1-\beta_i}} \right),$$

we have

$$x_i \sim q_i F_{0,i}^{\beta_i - 1}, \tag{3.8}$$
$$\frac{\partial x_i}{\partial q_i} \sim F_{0,i}^{\beta_i - 1},$$
$$\frac{\partial\, w_i F_i}{\partial q_i} \sim F_{0,i}^{\beta_i},$$

so we get

$$2(\Lambda \mathbf{q})_i = \lambda w_i F_{0,i}^{\beta_i},$$

(as before), subject to

$$\sum_{i=1}^{n} w_i \frac{F_{0,i}^{\beta_i}}{B_0} q_i = \log\left(\frac{K}{B_0}\right). \tag{3.9}$$

Notice that, *if* we linearize the right hand side we obtain again the constraint (3.5).

Now once again solving (3.4), $\mathbf{q} = \frac{1}{2}\lambda \Lambda^{-1} \widetilde{\mathbf{F}}_0$, but this time subject to the constraint (3.9), we find

$$\lambda = \frac{2B_0 \log\left(\frac{K}{B_0}\right)}{\widetilde{\mathbf{F}}_0^t \Lambda^{-1} \widetilde{\mathbf{F}}_0},$$

which plugged into (3.4) and using (3.8) yields

$$x_i = \frac{B_0 \log\left(\frac{K}{B_0}\right)}{\widetilde{\mathbf{F}}_0^t \Lambda^{-1} \widetilde{\mathbf{F}}_0} \left(\Lambda^{-1} \widetilde{\mathbf{F}}_0\right)_i F_{0,i}^{\beta_i - 1},$$

and this is easily seen to be identical to (3.1).

3.4. **Higher order approximations for the initial value.** We set

$$\mathbf{q} = \mathbf{q}_0 + \mathbf{q}_1, \tag{3.10}$$
$$\lambda = \lambda_0 + \lambda_1, \tag{3.11}$$

where $\mathbf{q}_0$ is given by (3.7) and λ_0 is given by (3.6). Inserting this into the expression (3.2), i.e.

$$(\Lambda \mathbf{q})_i = \frac{1}{2}\lambda w_i (F_{0,i}^{\beta_i} + \beta_i F_{0,i}^{2\beta_i - 1} q_i),$$

we get

$$(\Lambda(\mathbf{q}_0 + \mathbf{q}_1))_i = \frac{1}{2}(\lambda_0 + \lambda_1)\left(w_i F_{0,i}^{\beta_i} + w_i \beta_i F_{0,i}^{2\beta_i - 1}(q_{0,i} + q_{1,i})\right).$$

Letting, as before, $\widetilde{\mathbf{F}}$ and introducing the notation $(\widehat{\mathbf{F}})_i := w_i \beta_i F_{0,i}^{2\beta_i - 1}$, this may be written

$$\Lambda(\mathbf{q}_0 + \mathbf{q}_1) = \frac{1}{2}(\lambda_0 + \lambda_1)\left((\widetilde{\mathbf{F}} + \mathrm{Diag}(\widehat{\mathbf{F}})(\mathbf{q}_0 + \mathbf{q}_1)\right),$$

where "Diag" stands for a diagonal matrix. Since $\Lambda \mathbf{q}_0 = \frac{1}{2}\lambda_0 \widetilde{\mathbf{F}}$, we may drop two terms and this may be written

$$\Lambda \mathbf{q}_1 = \frac{1}{2}\lambda_0 (\mathrm{Diag}(\widehat{\mathbf{F}})(\mathbf{q}_0 + \mathbf{q}_1)) + \frac{1}{2}\lambda_1 (\mathrm{Diag}(\widehat{\mathbf{F}})(\mathbf{q}_0 + \mathbf{q}_1)) + \frac{1}{2}\lambda_1 \widetilde{\mathbf{F}}$$

Dropping the term involving $\lambda_1 \operatorname{Diag}((\widehat{\mathbf{F}}\mathbf{q}_1)$ we get:

$$\left(\Lambda - \frac{1}{2}\lambda_0 \operatorname{Diag}(\widehat{\mathbf{F}})\right)\mathbf{q}_1 = \frac{1}{2}\lambda_1 \operatorname{Diag}(\widehat{\mathbf{F}})\mathbf{q}_0 + \frac{1}{2}\lambda_0 \operatorname{Diag}(\widehat{\mathbf{F}})\mathbf{q}_0 + \frac{1}{2}\lambda_1\widetilde{\mathbf{F}},$$

which can be solved for

$$\begin{aligned}\mathbf{q}_1 = &\frac{1}{2}\lambda_1\left(\Lambda - \frac{1}{2}\lambda_0 \operatorname{Diag}(\widehat{\mathbf{F}})\right)^{-1} \operatorname{Diag}(\widehat{\mathbf{F}})\mathbf{q}_0\\ &+ \frac{1}{2}\lambda_1\left(\Lambda - \frac{1}{2}\lambda_0 \operatorname{Diag}(\widehat{\mathbf{F}})\right)^{-1}\widetilde{\mathbf{F}}\\ &+ \frac{1}{2}\lambda_0\left(\Lambda - \frac{1}{2}\lambda_0 \operatorname{Diag}(\widehat{\mathbf{F}})\right)^{-1} \operatorname{Diag}(\widehat{\mathbf{F}})\mathbf{q}_0\\ =:&\ \lambda_1\mathbf{G}_0 + \mathbf{H}_0.\end{aligned}$$

Similarly we rewrite the constraint

$$\sum w_i \cdot \left(F_0^i + F_{0,i}^{\beta_i} q_i + \frac{1}{2}\beta_i F_{0,i}^{2\beta_i - 1} q_i^2\right) = K$$

as

$$\sum w_i \left(F_{0,i}^i + F_{0,i}^{\beta_i}(q_{0,i} + q_{1,i}) + \frac{1}{2}\beta_i F_{0,i}^{2\beta_i-1}(q_{0,i}^2 + 2q_{0,i}q_{1,i} + q_{1,i}^2)\right) = K.$$

After using that by definition

$$\sum w_i \left(F_{0,i}^i + F_{0,i}^{\beta_i} q_{0,i}\right) = K$$

to cancel some terms, we get

$$\begin{aligned}0 = \sum w_i F_{0,i}^{\beta_i}(\lambda_1\mathbf{G}_0 + \mathbf{H}_0))_i +&\\ \frac{1}{2}w_i\beta_i F_{0,i}^{2\beta_i-1}\Big(q_{0,i}^2 + 2q_{0,i}(\lambda_1\mathbf{G}_0 + \mathbf{H}_0))_i + \frac{1}{2}(H_{0,i}^2 + 2\lambda_1 H_{0,i}G_{0,i} + \lambda_1^2 G_{0,i}^2)\Big).&\end{aligned}$$

This may be rewritten as:

$$\begin{aligned}\frac{1}{2}w_i\beta_i F_{0,i}^{2\beta_i-1}G_{0,i}^2\lambda_1^2 + \Big(\sum w_i F_{0,i}^{\beta_i}G_{0,i} + w_i\beta_i F_{0,i}^{2\beta_i-1}\left[q_{0,i}G_{0,i} + H_{0,i}G_{0,i}\right]\Big)\lambda_1&\\ + \sum w_i F_{0,i}^{\beta_i}H_{0,i} + \frac{1}{2}w_i\beta_i F_{0,i}^{2\beta_i-1}\left(2q_{0,i}H_{0,i} + \frac{1}{2}H_{0,i}^2\right) = 0.&\end{aligned}$$

Here we have two choices, we can drop the quadratic term in λ_1 or keep it, the first case leading to a linear equation and a corresponding λ_1^L and the second to a quadratic equation for the determination of λ_1^q.

4. The existence of the heat kernel expansion

When the diffusion matrix is non-degenerate and the domain is a compact manifold without a boundary, Yoshida [42], building on work of Minakshisundaram and Pleijel [32], [33], has shown how to use the so-called geometric series, which we recall in the appendix (A.2), as a starting point to obtain the *exact* fundamental solution to the backward Kolmogorov equation. The approach used by these authors has the drawback of being limited to compact domains and to non-degenerate diffusions. A probabilistic approach to the leading order behavior of a non-degenerate diffusion in small time was initiated by Varadhan [41]. This work was extended in several directions by Molchanov [34] and by Azencott and

collaborators [4] who also discuss the extension to the full zero-th order heat kernel coefficient for which a geometric interpretation in terms of Jacobi fields is given. In [5] the full heat kernel expansion is obtained on a domain of $\mathbf{R}^n$ using a stochastic Taylor expansion approach, under only the assumption of "local ellipticity" and C^∞ coefficients in the interior of the domain U. If the underlying Riemannian manifold is complete no additional assumptions need to be made. If on the other hand the underlying Riemannian manifold is incomplete it suffices that points x and y be sufficiently close compared with their distance to "infinity". More precisely when the underlying Riemannian manifold is incomplete, the heat kernel expansion still holds provided the condition

$$d(x,y) \leq d(x,\partial U) + d(y,\partial U) \tag{4.1}$$

is met (see [5], page 409, equation (6)). In the context of diffusions that degenerate on the boundary of the domain, the boundary may be at a finite distance from points in the interior, if the diffusions degenerate slowly at the boundary. This is the case for CEV diffusions, when $\beta_i < 1, i = 1,\ldots,n$. It is not assumed in Azencott's version that the domain is compact, but since the domain has a boundary, to insure uniqueness, he states his asymptotic results in reference to the so-called *minimal positive fundamental solution*, which at the boundary satisfies Dirichlet boundary conditions. The latter are indeed the mathematically correct boundary conditions for instance in the CEV case, when $\beta_i < 1$.

Ben Arous extended Azencott's results in [7] where he considers the hypoelliptic case on all of $\mathbf{R}^n$. Deuschel, Friz, Jacquier and Violante [13] have shown recently how Ben Arous's work can be extended in several directions thereby accommodating several financially interesting examples of hypoelliptic diffusions such as the Stein-Stein model. The multidimensional CEV model is however not hypoelliptic, so in our setting, the results of Azencott are the most directly relevant and indeed the Dirichlet boundary conditions are very reasonable from a financial point of view, since they correspond to bankruptcy, in case an asset's price reaches.

The main use of the above theoretical results in justifying the asymptotics in this paper, is in showing that the remainder in the heat kernel expansion, after the zero-th order term, is indeed $o(T)$ as $T \to 0$ on compact subsets of $\mathbf{R}^n_+ \times \mathbf{R}^n_+$. A crucial observation is that for the family of diffusions considered in this paper the cut locus is *empty*. This is due to the fact that, as shown at the beginning of Section A.2 in the Appendix, a diffeomorphism exists that maps the associated metric to *flat* metric (and hence establishes an isometry between the two).

We also can make use of the explicit form of the distance function (2.2), which shows, (since Λ is positive definite), that the latter grows quadratically in $\mathbf{q}$, so that, introducing the q_i's as new variables in (1.3), the exponential factor involving $\frac{-d^2}{2T}$ turns into a standard Gaussian. Moreover, as can be see from its explicit form (A.8), the u_0 heat kernel coefficient, in our setting, is the exponential of an at most linearly growing factor at infinity, provided that $\frac{\partial \sigma_i(F_i)}{\partial F_i}$ grows at most linearly at infinity. Although we do not carry out a complete proof here these elements are important building blocks in justifying the Laplace asymptotics used in deriving (2.8).

Remark 4.1. Since our multidimensional local volatility model is the image under a diffeomorphism of the x variables in which the metric is Euclidean, see Appendix A.2, and since sectional curvatures are invariant under a isometry and since the sectional curvatures in the Euclidean metric are all zero, the sectional curvatures of the image metric are still zero and therefore the cut locus in the new metric is empty as it was in the Euclidean case.

5. Numerical Results

In this section we present the numerical results. As mentioned in the introduction, one significant difference between the present work and most of the literature on asymptotics is the development and use of a highly accurate *benchmark* by which to gauge the accuracy of asymptotic expansions. In the past, most authors have used Monte Carlo or quasi Monte Carlo methods. Our finding, is however, that the accuracy in Monte Carlo, perhaps surprisingly, is not high enough.

Here we make use of the following techniques:

For computing the values of European options in the CEV model we are using the Ninomiya-Victoir method [35], a variant of the Kusuoka-Lyons-Victoir scheme (also known as cubature on Wiener space, see [26] and [29]). The Ninomiya-Victoir scheme is a second order weak approximation scheme for stochastic differential equations. We should mention here that the scheme requires smoothness of the driving vector fields of the stochastic differential equation. In the case of the CEV model, the vector fields are not differentiable at the boundary, i.e. when the underlying – or one component of the underlying – takes the value 0. Thus, when applying the Ninomiya-Victoir scheme to CEV or SABR type models, one should be aware of problems when the paths of the underlying frequently hit the boundary. When the underlying is, for instance, a portfolio of stocks, then the boundary behavior typically does not matter and one often empirically observes second order convergence, even though the exact regularity conditions are not satisfied, see [6]. On the other hand, for instance in SABR-LIBOR models, the boundary behavior will matter and one should not expect second order convergence any more. On a more technical side, we would like to remark that the Ninomiya-Victoir scheme requires us to solve the ODEs along the driving diffusion and Stratonovich-drift vector fields. In the case of a CEV or even a SABR model, [6] show that those ODEs can be solved explicitly, implying that these models are favorable for the Ninomiya-Victoir scheme in terms of efficiency.

As in the usual Euler scheme, the output of the Ninomiya-Victoir scheme is an n-dimensional random variable, $\overline{\mathbf{X}}$, which is a weak approximation to the underlying at the expiration date of the option – recall that n was the number of assets. Therefore, the Ninomiya-Victoir scheme needs to be coupled with an integration scheme in order to compute $E[f(\overline{\mathbf{X}})]$. We chose quasi Monte Carlo simulation (QMC) as integration scheme, based on Sobol numbers.

In addition, we were also using a variance reduction technique, known as *Mean Monte Carlo*, see [36], which is especially well suited for option pricing in multi-dimensional diffusion models. It is a variant of the control variate technique. In our case, for any single asset $1 \leq i \leq n$, we consider the n-dimensional random variable $\mathbf{X}_i$, which is defined by choosing all components $X_{i,l}$ constant except for $X_{i,i}$ which has a log-normal distribution with mean and variance chosen according to the corresponding CEV-parameters. Thus, the option price $E[f(\mathbf{X}_i)]$ is given explicitly by the Black-Scholes formula. Moreover, when the driving Brownian motion is equal to the driving Brownian motion of the ith component in the CEV model, then we can expect $\overline{\mathbf{X}}$ and $\mathbf{X}_i$ to be rather highly correlated. The control variate for $f(\overline{\mathbf{X}})$ is then a linear combination of the random variables $f(\mathbf{X}_1), \dots, f(\mathbf{X}_n)$ with coefficients chosen during the calculation so as to maximize the correlation.

In our empirical tests, we found that the Mean Monte Carlo method reduces the standard deviation by approximately 50%, thereby increasing the speed of calculation by a factor of four in a Monte Carlo setting. In our QMC framework, where the computational error is not governed by the standard deviation, it is not clear at the outset, whether a variance reduction technique can contribute to the efficiency of the integration scheme. In this

particular case, the numerical experiments seem to suggest that there is indeed a smaller integration error when combining QMC with the control variate described above, at the cost of negligible additional work.

Summing up, the reference "exact" values of the option prices were computed by discretization of the CEV stochastic differential equation using the Ninomiya-Victoir scheme together with quasi Monte-Carlo simulation with Mean Monte-Carlo simulation based on geometrical Brownian motion.

5.1. **Calculation of the optimal configuration (2.7).** Usually only three or four iterations are necessary for the optimal configuration to be obtained with a high degree of accuracy. For this reason, the optimal configuration can be viewed as given in closed form.

In order to deal with the constraint that the optimal configuration needs to lie on the hyperplane $\sum w_i F_i = K$, we can either eliminate one of the F_is and thus eliminate this constraint, or one can apply Newton's method to the augmented Lagrangian with a Lagrange multiplier to accommodate the constraint. One also needs to ensure that all components of the solution are non-negative.

In either case, it is desirable to provide Newton's method with a good starting point and so we have tested the various "warm start" points in section 3.1 both for their accuracy in providing a good approximation for the zero-th order implied volatility (2.16) and (2.18) and as a good starting point for Newton's method.

Note that in [3] the approximation (3.1) is used for the optimal configuration in the positive weight case. No attempt was reported to compute the optimal configuration with high precision. We find that (3.1) performs fairly well in the positive weight case and less so in the case with negative weights. Indeed it may even be undefined since it involves $\log\left(\frac{K}{B_0}\right)$, when $B_0 < 0$.

In practice, we recommend using the crude choice $\boldsymbol{F} = \boldsymbol{F}_0$ given in (3.7) together with the value λ of the Lagrange multiplier given in (3.6). This choice seems to combine robustness with fast convergence of Newton's iteration.

5.2. **Numerical results for first (and zero-th) order approximations.** As explained in the introduction to the numerics, highly accurate numerical simulation schemes with an estimated absolute statistical error of at most 10^{-4} were used to *benchmark* our asymptotic results. Such accuracy comes at a price, with certain computations running for more than a day, when the number of assets was greater than or equal to 5, and as long as a week, in the case of one hundred assets.

Somewhat surprisingly, although from a theoretical point of view the heat kernel method is only expected to provide a high degree of accuracy for relatively short maturities, here it performs well even for much longer times, but this accuracy does decrease with longer maturities, as illustrated in the examples presented below. Of course, the key quantities that need to be small are the dimensionless representative volatilities squared times the time to maturity $\sigma_i^2 T$. In our experiments we take volatilities of order $.1 - .9$, so that the dimensionless parameters, for instance for $T = 5$, are in the range $[.05, 4.05]$, in this case and in the range $[.01, .81]$ when $T = 1$.

T	$K = 16$	$K = 30$	$K = 32.1$	$K = 32.5$	$K = 39$	$K = 48$
0.5	16.0000	2.68949	1.48796	1.31129	0.09644	0.000770
1	16.0000	3.23769	2.11917	1.94345	0.38145	0.025389
2	16.0025	4.04471	3.00214	2.83018	1.00490	0.208926
5	16.0961	5.64629	4.70486	4.54272	2.54881	1.150898
10	16.4681	7.37418	6.51669	6.36644	4.38511	2.699937

TABLE 1. Quasi Monte Carlo prices for Example 5.1.

T	$K = 16$	$K = 30$	$K = 32.1$	$K = 32.5$	$K = 39$	$K = 48$
0.5	16.00000	2.06231	1.49089	1.31424	0.09737	0.000791
1	16.00001	2.67123	2.12746	1.95180	0.38645	0.026177
2	16.00265	3.54074	3.02542	2.85366	1.02440	0.217173
5	16.10517	5.26576	4.79485	4.63350	2.64063	1.220872
10	16.52356	7.18799	6.76048	6.61202	4.64883	2.945708

TABLE 2. Zero-order asymptotic prices for Example 5.1.

Example 5.1. The first numerical example concerns a basket option based on five assets. The correlation matrix used below is

$$\rho = \begin{pmatrix} 1 & 0.778051 & 0.154111 & 0.4783847 & 0.846901 \\ 0.778051 & 1 & -0.0835081 & 0.438172 & 0.483974 \\ 0.154111 & -0.0835081 & 1 & 0.778543 & 0.186014 \\ 0.478384 & 0.438172 & 0.778543 & 1 & 0.508852 \\ 0.846901 & 0.483974 & 0.186014 & 0.508852 & 1 \end{pmatrix},$$

while the other parameters are given by

$$\mathbf{F}_0 = (5,\ 6,\ 7,\ 6,\ 8)^t,$$
$$\beta = (0.5,\ 0.6,\ 0.2,\ 0.3,\ 0.9)^t,$$
$$\xi = (0.43969,\ 0.45080,\ 0.3837,\ 0.50290,\ 0.46548)^t.$$

Thus, the basket option is at-the-money when $K = 32$. Here, we compare the prices obtained from quasi Monte Carlo simulation with the zero order and first order asymptotic prices for strikes $K = 16,\ 30,\ 31.5,\ 32.1,\ 32.5,\ 39,\ 48$ and times to maturity of $T = 0.5,\ 1,\ 2,\ 5,\ 10$ years, see Tables 1, 2 and 3 below. We note that the simulation error for the "exact" prices given in Table 1 is at most of order 5×10^{-5} for $T = 0.5$, 7×10^{-5} for $T = 1$ and then increases in T. At $T = 10$, the error estimate is of order 1×10^{-3}. We see that the first order asymptotic prices are extremely precise, with errors not larger than 2×10^{-5} for our range of strike prices at $T = 0.5$ years and at $T = 1$ the error remains bounded by 1×10^{-4}. Even at $T = 5$ years, the errors of the first order asymptotic prices do not get larger than 2×10^{-3}. Even the zero-order prices are remarkably precise with errors of about 3×10^{-3} at $T = 0.5$ and 3×10^{-2} at $T = 2$, corresponding to a relative error of about 1%.

Figure 1 shows the "true" option prices in this example together with the first order approximation prices. As expected from the tables, the two lines for each maturity are visually indistinguishable, so that one can (almost) only see one line for each maturity T. In Figure 2 we show (on a logarithmic scale) the relative errors of the zeroth and first order approximate price formulas. For the zeroth order prices, the relative errors increase as the

T	$K = 16$	$K = 30$	$K = 32.1$	$K = 32.5$	$K = 39$	$K = 48$
0.5	16.00000	2.05953	1.48794	1.31127	0.09644	0.000771
1	16.00001	2.66325	2.11913	1.94338	0.38141	0.025387
2	16.00248	3.51803	3.00194	2.82989	1.00475	0.208924
5	16.09647	5.17648	4.70301	4.54045	2.54724	1.150153
10	16.46664	6.93932	6.50513	6.35319	4.37188	2.690597

TABLE 3. First order asymptotic prices for Example 5.1.

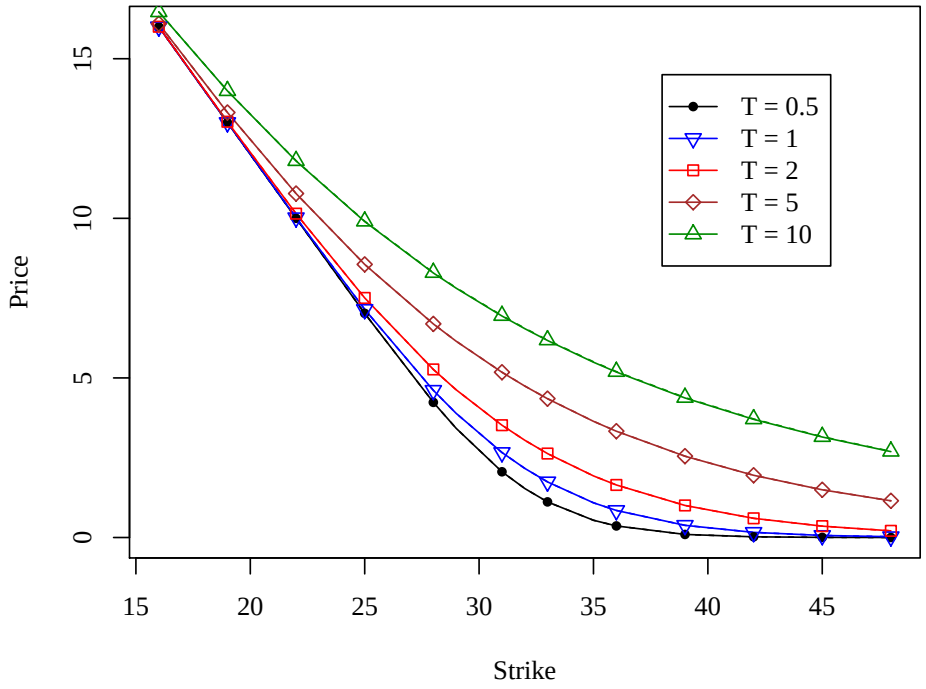

FIGURE 1. Exact and first order prices for Example 5.1. (Two lines are plotted for each maturity, corresponding to "exact" and first order prices, but they are visually indistinguishable.)

basket gets out of money, which is a simple consequence of dividing the absolute errors by smaller and smaller values (the corresponding exact option prices). For the first order prices, the same effect can be seen, but it is somewhat blurred by the erratic behaviour for small maturities, which is due to the Quasi Monte Carlo error, which is approximately of order 10^{-5} in this example – again subject to amplification far out of the money in relative terms. Comparing the first and zeroth order prices, we again see that the first order prices are roughly two orders of magnitude more exact.

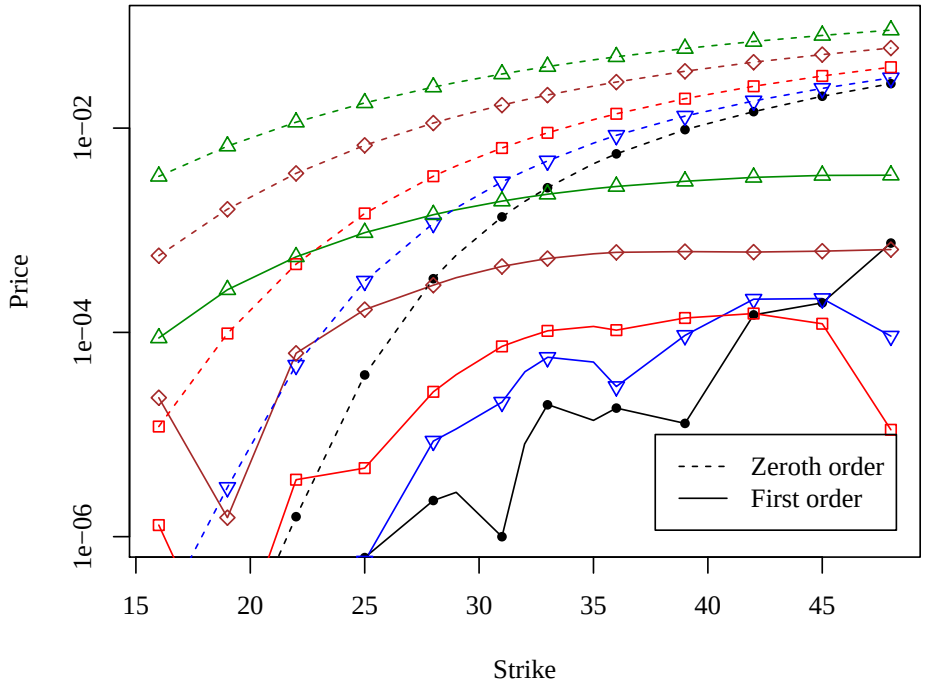

FIGURE 2. Relative errors for zeroth and first order approximate prices in Example 5.1. (For full legend compare with Figure 1.)

Example 5.2. Here we consider a generalized spread option based on 10 assets. The parameters are given by

$$\boldsymbol{\beta} = \begin{pmatrix} 0.7 \\ 0.2 \\ 0.8 \\ 0.3 \\ 0.5 \\ 0.5 \\ 0.6 \\ 0.6 \\ 0.3 \\ 0.3 \end{pmatrix}, \quad \boldsymbol{\xi} = \begin{pmatrix} 0.8 \\ 0.6 \\ 0.9 \\ 0.6 \\ 0.8 \\ 0.4 \\ 0.9 \\ 0.9 \\ 0.3 \\ 0.8 \end{pmatrix}, \quad \boldsymbol{F}_0 = \begin{pmatrix} 10 \\ 13 \\ 11 \\ 18 \\ 9 \\ 10 \\ 17 \\ 16 \\ 13 \\ 17 \end{pmatrix}, \quad \mathbf{w} = \begin{pmatrix} -1 \\ -1 \\ 1 \\ 1 \\ 1 \\ -1 \\ -1 \\ 1 \\ 1 \\ 1 \end{pmatrix}.$$

The entries of the correlation matrix

$$\rho = \begin{pmatrix} 1.00 & -0.22 & -0.10 & 0.02 & 0.01 & 0.00 & -0.00 & 0.00 & -0.00 & 0.00 \\ -0.22 & 1.00 & 0.47 & -0.08 & -0.06 & -0.01 & 0.01 & -0.00 & 0.00 & -0.00 \\ -0.10 & 0.47 & 1.00 & -0.18 & -0.14 & -0.02 & 0.01 & -0.00 & 0.00 & -0.00 \\ 0.02 & -0.08 & -0.18 & 1.00 & 0.77 & 0.14 & -0.08 & 0.03 & -0.00 & 0.00 \\ 0.01 & -0.06 & -0.14 & 0.77 & 1.00 & 0.18 & -0.10 & 0.03 & -0.00 & 0.00 \\ 0.00 & -0.01 & -0.02 & 0.14 & 0.18 & 1.00 & -0.58 & 0.18 & -0.02 & 0.02 \\ -0.00 & 0.01 & 0.01 & -0.08 & -0.10 & -0.58 & 1.00 & -0.32 & 0.03 & -0.03 \\ 0.00 & -0.00 & -0.00 & 0.03 & 0.03 & 0.18 & -0.32 & 1.00 & -0.10 & 0.10 \\ -0.00 & 0.00 & 0.00 & -0.00 & -0.00 & -0.02 & 0.03 & -0.10 & 1.00 & -0.96 \\ 0.00 & -0.00 & -0.00 & 0.00 & 0.00 & 0.02 & -0.03 & 0.10 & -0.96 & 1.00 \end{pmatrix}$$

are rounded to two digits for better readability. The full correlation matrix is, of course, available from the authors upon request. The parameters have been generated in a random way. In this case, the option is at-the-money at a strike of $K = 34$. We computed the option prices for strikes $K = 32.9,\ 33.5,\ 33.8,\ 34.1,\ 34.4,\ 34.7,\ 35.3$ and maturities of $T = 0.5,\ 1,\ 2,\ 5,\ 10$ years. The reference prices obtained by Monte-Carlo simulation are presented in Table 4. We note that the simulation error is smaller than 6×10^{-4} for $T = 0.5$ and smaller than 1×10^{-3} for $T = 1$ and increases to around 1×10^{-2} for $T = 10$. The first order asymptotic prices shown in Table 6 are of remarkable precision. At maturity $T = 0.5$ years the error is bounded by 1×10^{-4} throughout the whole range of strike prices. At maturity $T = 1$ years, the accuracy is still of the order 1.5×10^{-3}. Clearly, the accuracy decreases when the time to maturity increases. For the extremely large maturity of $T = 10$ years, the accuracy is around 4×10^{-1}. But even in this case, the relative error is only around 3%. The comparison to the zero order prices given in Table 5 show that the first order prices are substantially more accurate for maturities smaller than $T = 5$ years.

T	$K = 32.9$	$K = 33.5$	$K = 33.8$	$K = 34.1$	$K = 34.4$	$K = 34.7$	$K = 35.3$
0.5	3.6352	3.3143	3.1609	3.0123	2.8684	2.7292	2.4649
1	4.8959	4.5841	4.4332	4.2857	4.1416	4.0008	3.7292
2	6.6912	6.3870	6.2385	6.0924	5.9487	5.8074	5.5322
5	10.2656	9.9710	9.8261	9.6825	9.5408	9.4000	9.1251
10	14.2385	13.9482	13.8122	13.6726	13.5298	13.3877	13.1204

TABLE 4. Quasi Monte Carlo prices for Example 5.2.

T	$K = 32.9$	$K = 33.5$	$K = 33.8$	$K = 34.1$	$K = 34.4$	$K = 34.7$	$K = 35.3$
0.5	3.6306	3.3096	3.1562	3.0076	2.8637	2.7245	2.4601
1	4.8844	4.5724	4.4214	4.2739	4.1297	3.9890	3.7174
2	6.6640	6.3595	6.2109	6.0648	5.9211	5.7798	5.5046
5	10.2020	9.9069	9.7617	9.6182	9.4763	9.3361	9.0604
10	14.1930	13.9054	13.7635	13.6229	13.4835	13.3454	13.0728

TABLE 5. Zero order asymptotic prices for Example 5.2.

T	$K = 32.9$	$K = 33.5$	$K = 33.8$	$K = 34.1$	$K = 34.4$	$K = 34.7$	$K = 35.3$
0.5	3.6353	3.3143	3.1610	3.0123	2.8684	2.7292	2.4648
1	4.8976	4.5857	4.4348	4.2873	4.1431	4.0023	3.7307
2	6.7015	6.3972	6.2487	6.1027	5.9590	5.8177	5.5423
5	10.3507	10.0561	9.9112	9.7678	9.6260	9.4858	9.2100
10	14.6137	14.3277	14.1863	14.0461	13.9069	13.7689	13.4960

TABLE 6. First order asymptotic prices for Example 5.2.

Example 5.3. The next example is a basket based on 15 risky assets, with

$$\boldsymbol{\beta} = (0.7,\ 0.8,\ 0.9,\ 0.2,\ 0.4,\ 0.3,\ 0.3,\ 0.4,\ 0.4,\ 0.4,\ 0.1,\ 0.6,\ 0.5,\ 0.1,\ 0.2)^t,$$
$$\boldsymbol{\xi} = (0.6,\ 0.8,\ 0.1,\ 0.4,\ 0.4,\ 0.5,\ 0.4,\ 0.6,\ 0.9,\ 0.3,\ 0.3,\ 0.4,\ 0.5,\ 0.5,\ 0.5)^t,$$
$$\mathbf{F}_0 = (12,\ 11,\ 19,\ 15,\ 9,\ 13,\ 10,\ 12,\ 19,\ 12,\ 9,\ 9,\ 9,\ 10,\ 13)^t,$$

and weights $w_i \equiv 1$. Lack of space prevents us from giving the correlation matrix, which, as the other parameters, has been generated at random. Of course, it is available from the authors upon request. In contrast to the situation in Example 5.2, where the different assets were only lightly correlated, here, the average correlation between two assets is high at 68%. The option is at the money when the strike price satisfies $K = 182$. We present the "true" (Monte Carlo) prices (see Table 7) and the zero-order and first-order asymptotic prices (see Table 8 and 9, respectively) for times $T = 0.5$, $T = 1$ and $T = 2$ years and for strike prices $K = 178.5, 179.7, 180.9, 182.1, 183.3, 184.5, 185.7$. The simulation error is of order 5×10^{-4} for $T = 0.5$, 1×10^{-3} for $T = 1$ and 1.5×10^{-3} for $T = 2$. Again we see that, throughout a wide range of strike prices, the first-order asymptotic prices are almost exact up to order 10^{-4} for $T = 0.5$ years and still up to order 10^{-3} for $T = 1$ year. Even for $T = 2$, the first order asymptotic price has a surprising accuracy with errors of no more than 2×10^{-3} observed in our data. As no weight is negative, we are using the Black-Scholes version of the asymptotic prices.

T	$K = 178.5$	179.7	180.9	182.1	183.3	184.5	185.7
0.5	7.3631	6.6826	6.0442	5.4480	4.8935	4.3799	3.9063
1	9.5456	8.9029	8.2903	7.7078	7.1549	6.6310	6.1357
2	12.6380	12.0280	11.4395	10.8724	10.3264	9.8011	9.2963

TABLE 7. Quasi Monte Carlo prices for Example 5.3.

T	$K = 178.5$	179.7	180.9	182.1	183.3	184.5	185.7
0.5	7.3738	6.6937	6.0555	5.4593	4.9047	4.3909	3.9172
1	9.5760	8.9339	8.3218	7.7394	7.1864	6.6625	6.1672
2	12.7233	12.1144	11.5269	10.9605	10.4149	9.8900	9.3854

TABLE 8. Zero-order asymptotic prices for Example 5.3.

T	$K = 178.5$	179.7	180.9	182.1	183.3	184.5	185.7
0.5	7.3633	6.6829	6.0445	5.4481	4.8934	4.3797	3.9061
1	9.5456	8.9030	8.2904	7.7077	7.1545	6.6305	6.1352
2	12.6369	12.0269	11.4383	10.8710	10.3247	9.7993	9.2943

TABLE 9. First-order asymptotic prices for Example 5.3.

Example 5.4. In a second 15-dimensional example, we present the case of a high-dimensional generalized spread option. The parameters are this time given by

$$\boldsymbol{\beta} = (0.3,\ 0.1,\ 0.1,\ 0.8,\ 0.8,\ 0.5,\ 0.6,\ 0.4,\ 0.8,\ 0.4,\ 0.9,\ 0.2,\ 0.1,\ 0.8,\ 0.4)^t,$$
$$\boldsymbol{\xi} = (0.7,\ 0.7,\ 0.4,\ 0.4,\ 0.8,\ 0.5,\ 0.1,\ 0.5,\ 0.4,\ 0.9,\ 0.6,\ 0.4,\ 0.5,\ 0.5,\ 0.5)^t,$$
$$\mathbf{F}_0 = (10,\ 8,\ 15,\ 13,\ 13,\ 9,\ 18,\ 15,\ 13,\ 9,\ 12,\ 19,\ 11,\ 11,\ 13)^t,$$
$$\mathbf{w} = (1,\ 1,\ 1,\ -1,\ -1,\ -1,\ 1,\ 1,\ -1,\ 1,\ -1,\ -1,\ 1,\ 1,\ 1)^t.$$

Again, we stress that the parameters have been chosen at random, and lack of space prevents us from giving the correlation matrix $\boldsymbol{\rho}$, which is naturally available from the authors upon request. Similarly to Example 5.3, the assets are on average highly correlated with an average correlation of 60%. This time, the option is at the money when $K = 31$. We give the "exact" prices of the spread options for time to maturity $T = 0.5$, $T = 1$ and $T = 2$ years and for strike prices $K = 27.5, 28.7, 29.9, 31.1, 32.3, 33.5, 34.7$. The simulation error in Table 10 is at $T = 1$ bounded by 5×10^{-4}, by 3×10^{-4} at $T = 0.5$ and by 7×10^{-4} at $T = 2$. The zero order prices are reported in Table 11 and the first order prices in Table 12. In this case, some weights are negative, so we use the Bachelier version of the asymptotic pricing formulas. We again observe extremely good fit for the first order prices, of order 10^{-4} for $T = 0.5$ years and 5×10^{-4} at $T = 1$. At $T = 2$, the fit is still satisfactory with 3×10^{-3}. Surprisingly, this time the zero-order prices are of similar quality, at least for in-the-money strike prices K. In fact, at $T = 2$ they seem to be convincingly closer to the exact prices than the first order asymptotic prices in the money.

T	$K = 27.5$	$K = 28.7$	$K = 29.9$	$K = 31.1$	$K = 32.3$	$K = 33.5$	$K = 34.7$
0.5	4.8596	4.0101	3.2333	2.5373	1.9293	1.4137	0.9919
1	5.9055	5.0862	4.3191	3.6092	2.9608	2.3781	1.8641
2	7.4510	6.6379	5.8614	5.1247	4.4308	3.7828	3.1839

TABLE 10. Quasi Monte Carlo prices for Example 5.4

T	$K = 27.5$	$K = 28.7$	$K = 29.9$	$K = 31.1$	$K = 32.3$	$K = 33.5$	$K = 34.7$
0.5	4.8598	4.0101	3.2331	2.5369	1.9286	1.4128	0.9909
1	5.9062	5.0864	4.3188	3.6082	2.9592	2.3759	1.8613
2	7.4543	6.6397	5.8617	5.1233	4.4277	3.7778	3.1769

TABLE 11. Zero order prices for Example 5.4.

Example 5.5. As an especially challenging example, we also computed prices of a 100-dimensional basket option, i.e. of a European call option on an index based on 100 stocks. We cannot present the precise parameters in this paper any more, but clearly they are

T	$K = 27.5$	$K = 28.7$	$K = 29.9$	$K = 31.1$	$K = 32.3$	$K = 33.5$	$K = 34.7$
0.5	4.8597	4.0103	3.2334	2.5374	1.9293	1.4137	0.9919
1	5.9061	5.0867	4.3197	3.6097	2.9613	2.3785	1.8645
2	7.4539	6.6407	5.8642	5.1274	4.4335	3.7854	3.1863

TABLE 12. First order prices for Example 5.4.

available from the authors upon request. As before, the parameters have been generated in a random way. The "volatilities" ξ_i range between 0.48 and 0.59, with mean volatility 0.52. The correlation between different assets are very high, their mean value being 76%. The β_i vary between a minimum value of 0.12 and a maximum value of 0.99 with a mean value of 0.52. The initial forward prices take values between 3.03 and 6.99 with a mean value of 5.05, implying that the option is at-the-money at a strike $K = 504.6$. We report the different prices for strikes $K = 502, 503.2, 503.6, 504, 504.4, 504.8, 505.2$. Due to the prohibitive running time of the simulation algorithm, the simulation error is at most of order 10^{-2} in Table 13. We note that the error of the first order asymptotic formula, see Table 15, is mostly smaller than 10^{-2}, i.e., the first order asymptotic error is within the accuracy bounds obtained from the simulation algorithm. The zero-order asymptotic formula, see Table 14, however, can be quite far away from the true price.

T	$K = 502$	503.2	503.6	504	504.4	504.8	505.2
0.5	34.018	33.433	33.245	33.057	32.869	32.678	32.483
1	47.390	46.834	46.650	46.466	46.280	46.101	45.924

TABLE 13. Quasi Monte Carlo prices for Example 5.5.

T	$K = 502$	503.2	503.6	504	504.4	504.8	505.2
0.5	34.090	33.513	33.323	33.133	32.944	32.756	32.568
1	47.614	47.056	46.871	46.686	46.502	46.319	46.136

TABLE 14. Zero order prices in Example 5.5.

T	$K = 502$	503.2	503.6	504	504.4	504.8	505.2
0.5	34.013	33.437	33.246	33.057	32.868	32.680	32.492
1	47.399	46.841	46.656	46.471	46.288	46.104	45.921

TABLE 15. First order prices in Example 5.5.

5.3. **Summary of numerical results.** We conclude the section on numerical experiments by two summarizing tables, in which we report the ratio between the relative errors for the zero-order prices and the first order prices, respectively, to the dimension-free time to maturity "$\sigma^2 T$". In the case of a basket-option, we clearly have to choose some appropriate average volatility $\overline{\sigma}$ for σ. We think that the most appropriate choice in our multi-dimensional CEV framework is

$$\overline{\sigma} = \frac{\sigma_{\mathcal{N},\mathcal{B}}(\mathbf{F}_0)}{\sum_{i=1}^n w_i F_{0,i}},$$

T	Ex. 5.1	Ex. 5.2	Ex. 5.3	Ex. 5.4
0.5	0.1555	−0.0293	0.3085	−0.0143
1	0.1481	−0.0261	0.3162	−0.0105
2	0.1429	−0.0218	0.3222	−0.0075
5	0.1376	−0.0129	0.3252	
10	0.1328	−0.0035	0.3198	
$\overline{\sigma}$	0.1704	0.3187	0.1073	0.2964

TABLE 16. Normalized error of the zero-order asymptotic prices.

T	Ex. 5.1	Ex. 5.2	Ex. 5.3	Ex. 5.4
0.5	-4.02×10^{-4}	1.76×10^{-4}	8.76×10^{-3}	5.06×10^{-5}
1	-9.47×10^{-4}	3.58×10^{-3}	1.53×10^{-3}	2.08×10^{-3}
2	-1.63×10^{-3}	8.09×10^{-3}	-3.92×10^{-3}	3.89×10^{-3}
5	-3.41×10^{-3}	1.71×10^{-2}	-1.33×10^{-2}	
10	-7.15×10^{-3}	2.67×10^{-2}	-2.82×10^{-2}	
$\overline{\sigma}$	0.1704	0.3187	0.1073	0.2964

TABLE 17. Normalized error of the first order asymptotic prices.

where we normalize in order to obtain a log-normal volatility. For each of the Examples 5.1, 5.2, 5.3 and 5.4 we report that ratio over all times of maturity T, but only for one representative strike price K. In the case of Example 5.1, we choose $K = 32.5$, for Example 5.2 we choose $K = 33.8$, for Example 5.3 we take $K = 180.3$ and, finally, for Example 5.4 we consider $K = 33.5$.

Apart from the general observation, that the normalized errors of the zero-order prices are generally much larger than the normalized errors of the first order prices, we see that the normalized errors for the zero-order prices are more-or-less constant in T, implying that the zero-order prices converge with rate T to the true prices as $T \to 0$. On the other hand, the normalized relative errors of the first order prices seem to roughly double when T doubles. Consequently, the first order prices seem to converge to the true prices with rate T^2, convincingly so for Examples 5.1, 5.2 and, to some extent, 5.4. Thus, the numerical example convincingly reconfirm the results of the asymptotic analysis. Even more, in some cases it seems that $T = 10$ is already in the asymptotic regime.

Finally, we would also like to compare our results to the classical results by Avellaneda et al. [3], who are using a slightly different approach. Indeed, they use a heat kernel expansion to derive a local volatility for the basket from the local volatilities of the individual components, and then obtain the implied volatility by the "1/2-slope rule", see Gatheral [16], i.e. as the average local volatility at the initial and the minimizing configuration. In Table 18, we report the relative errors of our zero-order price – denoted by σ_0

	$K = 178.5$	179.7	182.1	183.3	184.5	185.7
σ_0	0.00146	0.00166	0.00208	0.00229	0.00253	0.00279
σ_{AV}	0.00147	0.00167	0.00208	0.00229	0.00254	0.00281
$\sigma_{0,AV}$	0.00639	0.00535	0.00188	−0.00071	−0.00392	−0.00784

TABLE 18. Comparison of 0 order prices with prices obtained in [3]. Relative errors in Example 5.3 for $T = 0.5$.

in the table – and the price obtained from the implied volatility of [3] – denoted by σ_{AV} in the table. Finally, we also present the results that we would obtain if we directly used their approximation of the minimizing configuration for our zero order formula, instead of just as a starting value for a Newton iteration – denoted by $\sigma_{0,AV}$ in the table. The degree of agreement between our zero order prices and the prices of Avellaneda et al. is quite astonishing, whereas the quality is certainly considerably worse if we replace the minimizing configuration by its approximation. So it seems that the "1/2-slope trick" effectively allows one to avoid the (completely unproblematic) Newton iteration, at no cost of precision. The first order approximation is, in this case, by almost two orders of magnitude better in terms of the relative error than either our zero order price or the price obtained by Avellaneda et al.

6. Future Work

A big challenge is to devise models which consistently price both the basket option and its components, in the presence of a skew, such as the one found in equity markets. The model considered does allow a reasonable level of skew in both components and in the basket, as illustrated by an example in Figure 3. An additional feature, as was pointed out by the referee, to incorporate into the local vol basket model, is time inhomogeneous volatilities and correlations. This is quite straightforward to do, following the approach in [17], where the time dependent coefficients are expanded in a Taylor series around the initial time t. However, since Taylor expansions are used, such expansions can only be expected to be effective for relatively short dated options. An interesting alternative is to combine the present approach with one of the more sophisticated "global" approaches to time dependent coefficients, such as the approaches of Reghai [38], Guyon and Henry-Labordère [20], or that of Gatheral and Wang [18]. It is also desirable to extend the present work to local volatility models in which the correlations exhibit state-dependence. These have been termed "local correlation models".

Appendix A. Heat kernel expansions for local volatility models

A.1. **Heat kernel expansion.** Given a linear variable coefficient parabolic partial differential equation

$$u_t + \frac{1}{2}a^{ij}u_{x_ix_j} + b^i u_{x_i} = 0. \tag{A.1}$$

In the time homogeneous case, we may without loss of generality assume the initial time is 0. It is well-studied in differential geometry and stochastic analysis that under certain technical conditions (see e.g. [42], [12]) the transition density has, in the time homogeneous case, the following family of N-th order approximations p_N,

$$p_N(\mathbf{x}_0;\mathbf{x},T) = \sqrt{g(\mathbf{x})}U_N(\mathbf{x}_0;\mathbf{x},T)\frac{e^{-\frac{d^2(\mathbf{x}_0,\mathbf{x})}{2T}}}{(2\pi T)^{\frac{n}{2}}} \tag{A.2}$$

where,

- g is the volume form associated with the Riemannian metric determined by $\mathbf{g}$, the inverse of the diffusion matrix a^{ij}. The inner product, denoted $\langle .,. \rangle$, of two tangent vectors $\mathbf{A}$ and $\mathbf{B}$ is, in local coordinates given by
$$\langle \mathbf{A}, \mathbf{B} \rangle = g_{ij}A_iB_j,$$
where the Einstein summation is used to sum over repeated indices.

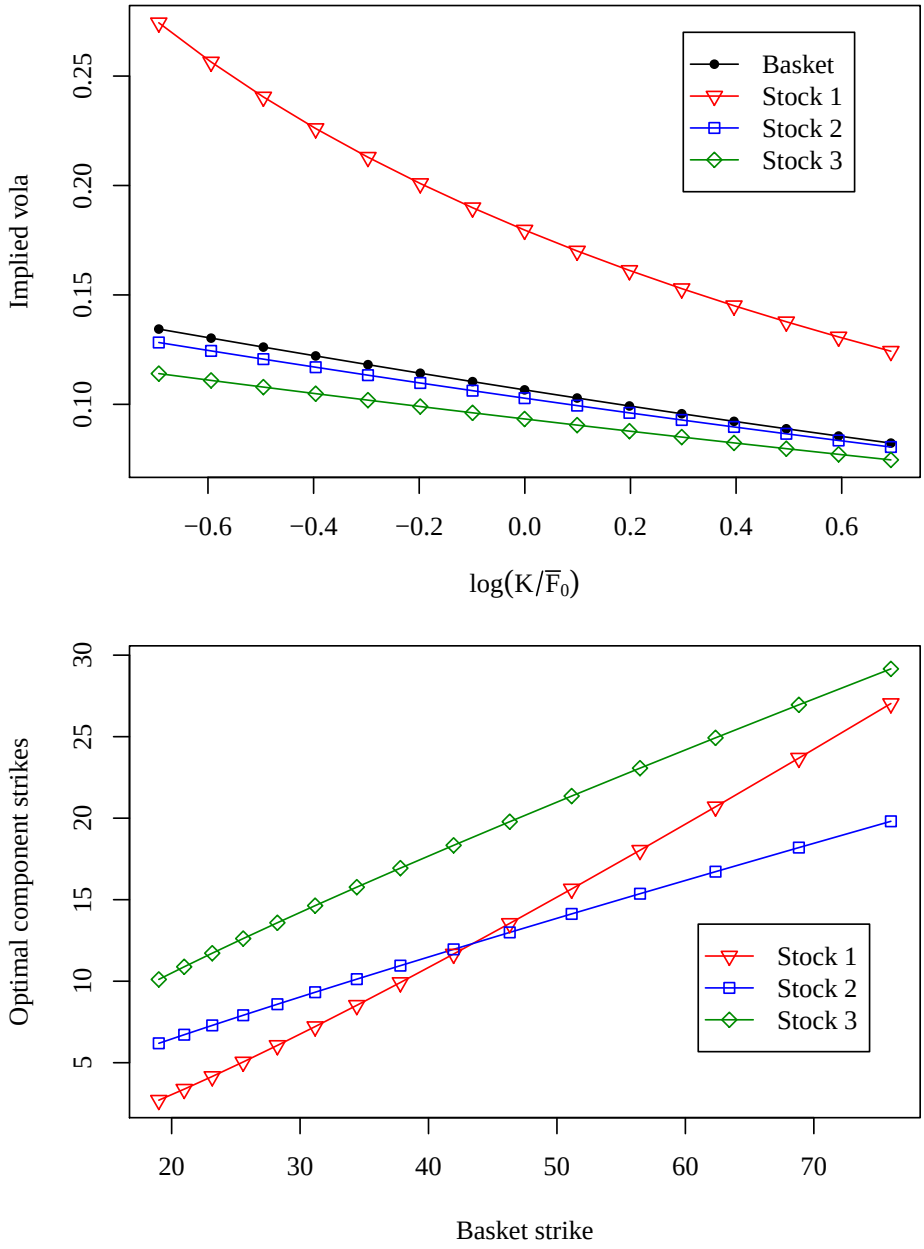

FIGURE 3. Implied volas of a basket of three assets and the implied volas of the individual components. In the top plot, the implied vola for the basket option is plotted together with the implied volas of the individual components *at the optimal configuration*, i.e., at strikes $\mathbf{F}^\star$. In the bottom plot, the optimal configuration $\mathbf{F}^\star$ is plotted against the strike of the basket. Parameters: $\mathbf{F}_0 = (10, 11, 17)$, $\boldsymbol{\beta} = (0.3, 0.2, 0.2)$, $\boldsymbol{\xi} = (0.9, 0.7, 0.9)$, $\rho_{12} = 0.8$, $\rho_{13} = 0.7$, $\rho_{23} = 0.6$.

- $d(\mathbf{x}_0, \mathbf{x})$ is the geodesic (Riemannian) distance between $\mathbf{x}_0$ and $\mathbf{x}$, in the above mentioned metric g_{ij} corresponding to the inverse of the diffusion matrix.
- U_N is given by the series expansion:

$$U_N(\mathbf{x}_0; \mathbf{x}, T) = \sum_{k=0}^{N} u_k(\mathbf{x}_0; \mathbf{x}) T^k. \tag{A.3}$$

  The u_k's are called the heat kernel coefficients. In particular, $u_0(\mathbf{x}_0; \mathbf{x}) = \sqrt{\Delta(\mathbf{x}_0, \mathbf{x})} e^{\int_\gamma \langle V, \dot{\gamma} \rangle}$, where Δ and V are defined below.
- Δ is the Van Vleck-DeWitt determinant:

$$\Delta(\mathbf{x}_0, \mathbf{x}) = \frac{1}{\sqrt{g(\mathbf{x}_0) g(\mathbf{x})}} \det\left(-\frac{1}{2} \frac{\partial^2 d^2}{\partial \mathbf{x}_0 \partial \mathbf{x}} \right).$$

- $\mathcal{P} = e^{\int_\gamma \langle V, \dot{\gamma} \rangle}$ is the exponential of the work done by the vector field V along the geodesic γ, joining $\mathbf{x}_0$ to $\mathbf{x}$, with $V = V^i \partial_i$ and

$$V^i = b^i - \frac{1}{2\sqrt{g}} \frac{\partial}{\partial x^j} \left[\sqrt{g} g^{ij} \right], \tag{A.4}$$

  where $\mathbf{b}$ is the drift in PDE (A.1).

We refer to the expansion (A.2) of order N as the *geometric expansion* of order N. This terminology is motivated by the fact that the expansion contains terms that are obtained using geometric information such as the geodesics. It is important to note that the geometric expansion is an asymptotic one and not a convergent one. In the classical treatment, p_N in [42], p_N is multiplied by a test function that localizes the expansion sufficiently close to the diagonal.In this paper what is needed to justify the asymptotics is that $\hat{p}_N$ provides an asymptotic expansion of order N, i.e., if we denote by p the exact transition density, then we have

$$\lim_{T \to 0} \frac{\hat{p}_N(\mathbf{x}, \mathbf{y}, T) - p(\mathbf{x}, \mathbf{y}, T)}{T^N} = 0, \quad \forall N \in \mathrm{N}$$

uniformly on compact sets, away from the cut locus. Since our metric is flat, the cut locus in in fact empty. Using the asymptotics equivalence relation $\sim$ we have

$$p(\mathbf{x}, \mathbf{y}, T) - \hat{p}_N(\mathbf{x}, \mathbf{y}, T) \sim o(T^N), \quad \text{as } T \to 0$$

These estimates are indeed availables, in a variety of contexts, as illustrated by equation (4) in Theorems 1.2 and 1.3 in [5] and Theorem (3.1) in [7].

Remark A.1. Care needs to be taken to adhere to the following *convention* when integrating along the geodesic: The *starting point* is the backward point $\mathbf{x}_0$ and the endpoint is $\mathbf{x}$. Some authors prefer to integrate from the endpoint to the starting point, in which case V must be replaced by $-V$.

By adding and subtracting first order terms, (A.1) can then be re-expressed in the form

$$u_t + \frac{1}{2} \Delta_B u + V \cdot \nabla u = 0, \tag{A.5}$$

where Δ_B is the second order Laplace Beltrami operator $\frac{1}{\sqrt{g}} \frac{\partial}{\partial x_i} (\sqrt{g} g^{ij} \frac{\partial}{\partial x_j})$.

Note that the zeroth order heat kernel coefficient is known in closed form provided we have available in closed form both the distance function and the geodesics. The higher order on diagonal heat kernel coefficients $u_i(\mathbf{x}, \mathbf{x})$ have been calculated up to order 4 in very general settings. On the other hand the efficient calculation of the *off diagonal* heat

kernel coefficients u_i, for $i \geq 1$, is still an active field of research. We refer to Hsu [24] for an in-depth introduction to heat kernel expansion from a stochastic analysis perspective.

Given the heat kernel expansion in (A.2) for the transition density p, the call price C as $T \to 0^+$ has an expansion obtained by inserting the geometric series into (1.3).

A.2. **Action Integral.** In order to isolate the covariant form of the drift to be used in the action integral, one can proceed directly in the original coordinates as in [8] or alternatively by making changes of variables and exploiting the invariance of the form $\int \mathcal{A} \cdot \mathbf{dl}$ under changes of variables. Here we do the latter. i.e., beginning with

$$u_t + \frac{1}{2}\rho_{ij}\sigma_i(F_i)\sigma_j(F_j)u_{F_iF_j} = 0,$$

we set

$$y_i = \int_0^{F_i} \frac{1}{\sigma_i(u)}du. \tag{A.6}$$

Then with $v(y_1, \ldots, y_n, t) = u(F_1(y_1), \ldots, F_n(y_n), t)$, using

$$u_{F_i} = v_{y_i}\frac{1}{\sigma_i(F_i)},$$
$$u_{F_iF_j} = v_{y_iy_j}\frac{1}{\sigma_i(F_i)\sigma_j(F_j)} - \delta_{ij}v_{y_i}\frac{(\sigma_i)'(F_i)}{(\sigma_i)^2},$$

we see that v satisfies the pde

$$v_t + \frac{1}{2}\rho_{ij}v_{y_iy_j} - \frac{1}{2}(\sigma_i)'v_{y_i} = 0.$$

Last we let L be a matrix that conjugates ρ to the identity, i.e. $L\rho L^t = Id$,[3]

$$x_i = L_{ip}y_p,$$
$$v(y_1, \ldots, y_n, t) = w(x_1, \ldots, x_n, t),$$
$$v_{y_i} = w_{x_k}L_{ki}, \quad v_{y_iy_j} = w_{x_kx_l}L_{ki}L_{lj},$$
$$\rho_{ij}v_{y_iy_j} = L_{ki}\rho_{ij}L_{lj}w_{x_kx_l} = \text{Trace}(L\rho L^t\,\text{Hessian}(w)) = w_{x_ix_i}.$$

So the final equation is

$$w_t + \frac{1}{2}w_{x_ix_i} - \frac{1}{2}L_{ik}(\sigma_k)'(F_k)w_{x_i} = 0.$$

The transformation from $\mathbf{F}$ to $\mathbf{x}$ is $x_i = L_{ik}\int_0^{F_i}\frac{1}{\sigma_i(u)}du$. So, we see that the covariant drift that we need to integrate along the geodesics which are straight lines is $-\frac{1}{2}L_{ik}(\sigma_k)'(F_k)$. The 1-form is thus given by

$$-\frac{1}{2}L_{ik}(\sigma_k)'(F_k)dx^i =: \mathcal{A}_i^x dx^i. \tag{A.7}$$

Alternatively, this term may also be expressed in the original variables in the form

$$\mathcal{A}_i^F dF^i = -\frac{1}{2}\Lambda\frac{\frac{\partial\sigma_j(F_j)}{\partial F_j}}{\sigma_i(F_i)}dF_i \tag{A.8}$$

[3]Cholesky decomposition furnishes one approach to get L and diagonalization another.

A.2.1. *Geometric Brownian motion case.* In the case of a geometric Brownian motion, we have

$$(\sigma_k)'(F_k) = \sigma_k,$$
$$y_k = \frac{1}{\sigma_k}\log(F_k).$$

Now in the $\mathbf{x}$ plane, geodesics are straight lines joining the points $\mathbf{x}_0$ and $\mathbf{x}_1$ which are the images under the transformations above of the points $\mathbf{F}_0$ and $\mathbf{F}_1$ respectively. So, parametrizing an arbitrary point $\mathbf{x}_0 + \lambda(\mathbf{x}_1 - \mathbf{x}_0)$ on this line segment by λ, we note that arc length is given by $|\mathbf{x}_1 - \mathbf{x}_0|d\lambda = c_{\mathbf{x}_0,\mathbf{x}_1}d\lambda$. Therefore, letting $\boldsymbol{\sigma}$ be the vector with entries σ_k, we have

$$\begin{aligned}\int \mathcal{A}_i dx^i &= -\frac{1}{2}\int_{\gamma(x_0,x_1)} L_{ik}\sigma_k dx^i \\ &= -\frac{1}{2}\int_0^1 \sigma_k L_{ik}(x_1 - x_0)_i d\lambda \\ &= \sigma_k L_{ik}L_{ip}\frac{1}{\boldsymbol{\sigma}_p}\log\left(\frac{F_p}{F_{0,p}}\right) \\ &= -\frac{1}{2}\boldsymbol{\sigma}\log\left(\frac{\mathbf{F}}{\mathbf{F}_0}\right)^t \rho^{-1}\frac{1}{\boldsymbol{\sigma}}, \qquad \text{(A.9)}\end{aligned}$$

which has to be interpreted liberally in the sense of the previous term. In the above expression we clearly recognize the constant (in T) part of the exponent of the lognormal distribution (with arbitrary volatilities)

$$\frac{1}{(2\pi T)^{\frac{n}{2}}\sigma_1 F_1 \dots \sigma_n F_n|\rho|^{\frac{1}{2}}} e^{-\frac{(\log(\frac{\mathbf{F}}{\mathbf{F_0}})+\frac{1}{2}\boldsymbol{\sigma}^2 T)^t\Sigma^{-1}(\log(\frac{\mathbf{F}}{\mathbf{F_0}})+\frac{1}{2}\boldsymbol{\sigma}^2 T)}{2T}} dF_1 \dots dF_n.$$

A.2.2. *CEV case.* Let us suppose $\sigma_k(F_k) = \xi_k F_k^{\beta_k}$ so $\sigma_k'(F_k) = \xi_k\beta_k F_k^{\beta_k - 1}$. Notice that in this case we have, since $y_k = \frac{1}{(1-\beta_k)\xi_k}F_k^{1-\beta_k}$,

$$\sigma_k'(F_k) = \frac{\beta_k}{1-\beta_k}\frac{1}{y_k} = \frac{\beta_k}{1-\beta_k}\frac{1}{(L^{-1})_{kj}x_j}.$$

Therefore by simple manipulations we get

$$\int_{\gamma(\mathbf{x}_0,\mathbf{x}_1)} \mathcal{A}_i dx^i = -\frac{1}{2}\log\left(\frac{a_k + b_k}{a_k}\right)\frac{\beta_k\xi_k}{b_k(1-\beta_k)}(\rho^{-1})_{kp}\frac{1}{\xi_p(1-\beta_p)}(F_p^{1-\beta_p} - F_{0,p}^{1-\beta_p}), \qquad \text{(A.10)}$$

where we have set

$$\mathbf{a} = L^{-1}\mathbf{x}_0 = L^{-1}L\frac{1}{1-\boldsymbol{\beta}}\frac{1}{\boldsymbol{\xi}}\mathbf{F}_0^{1-\boldsymbol{\beta}} = \frac{1}{\boldsymbol{\xi}(1-\boldsymbol{\beta})}\mathbf{F}_0^{1-\boldsymbol{\beta}},$$
$$\mathbf{b} = L^{-1}(\mathbf{x}_1 - \mathbf{x}_0) = L^{-1}L\frac{1}{\boldsymbol{\xi}(1-\boldsymbol{\beta})}(\mathbf{F}^{1-\boldsymbol{\beta}} - \mathbf{F}_0^{1-\boldsymbol{\beta}}) = \frac{1}{\boldsymbol{\xi}(1-\boldsymbol{\beta})}(\mathbf{F}^{1-\boldsymbol{\beta}} - \mathbf{F}_0^{1-\boldsymbol{\beta}}),$$
$$a + b = \frac{1}{\boldsymbol{\xi}(1-\boldsymbol{\beta})}\mathbf{F}^{1-\boldsymbol{\beta}},$$

so that (A.10) can be written

$$-\frac{1}{2}(1-\beta_k)\log\left(\frac{F_k}{F_{0,k}}\right)\frac{\beta_k\xi_k}{F_k^{1-\beta_k} - F_{0,k}^{1-\beta_k}}(\rho^{-1})_{kp}\frac{1}{\xi_p(1-\beta_p)}(F_p^{1-\beta_p} - F_{0,p}^{1-\beta_p}).$$

Note that in the limit $\beta_k \to 1, \forall k$, we have by L'Hospital's rule that $\frac{1}{1-\beta_k}(F_k^{1-\beta_k} - F_{0,k}^{1-\beta_k}) \to \log(\frac{F_k}{F_{0,k}})$. Hence it is easily seen that we recover the lognormal result (A.9) in this limit.

References

[1] Alexander, C.; Venkatramanan, A. Analytic approximations for multi-asset option pricing. *Mathematical Finance* (2011), no–no. Available at: http://dx.doi.org/10.1111/j.1467-9965.2011.00481.x

[2] Alos, E.; Eydeland, A.; Laurence, P. A Kirk's and a Bachelier formula for three asset spread options. *Energy risk* (2011).

[3] Avellaneda, M.; Boyer-Olson, D.; Busca, J.; Friz, P. Application of large deviation methods to the pricing of index options in finance. *C. R. Math. Acad. Sci. Paris* **336** (2003), no. 3, 263–266. Available at: http://dx.doi.org/10.1016/S1631-073X(03)00032-3

[4] Azencott, R. *Géodésiques et diffusions en temps petit*, *Astérisque*, vol. 84, Société Mathématique de France, Paris, 1981. Probability Seminar, University of Paris VII, Paris.

[5] Azencott, R. Densité des diffusions en temps petit: développements asymptotiques. I. in *Seminar on probability, XVIII*, *Lecture Notes in Math.*, vol. 1059, pp. 402–498, Springer, Berlin, 1984. Available at: http://dx.doi.org/10.1007/BFb0100057

[6] Bayer, C.; Friz, P.; Loeffen, R. Semi-closed form cubature and applications to financial diffusion models. 2011. Preprint.

[7] Ben Arous, G. Développement asymptotique du noyau de la chaleur hypoelliptique hors du cut-locus. *Ann. Sci. École Norm. Sup. (4)* **21** (1988), no. 3, 307–331. Available at: http://www.numdam.org/item?id=ASENS_1988_4_21_3_307_0

[8] Ben Arous, G.; Laurence, P. Second order expansion for implied volatility in two factor local-stochastiv volatility models and applications to the dynamic λ-sabr model. 2010. Preprint.

[9] Bjerksund, P.; Stensland, G. Closed form spread option valuation. *Quantitative Finance* **0** (0), no. 0, 1–10. Available at: http://www.tandfonline.com/doi/abs/10.1080/14697688.2011.617775

[10] Carmona, R.; Durrleman, V.: Pricing and hedging basket options in a log-normal model, Tech. rep., Department of Operations Research and Financial Engineering, Princeton University. 2003.

[11] Carmona, R.; Durrleman, V. Pricing and hedging spread options. *SIAM Review* **45** (2003), no. 4, pp. 627–685.

[12] Chavel, I. *Eigenvalues in Riemannian geometry*, *Pure and Applied Mathematics*, vol. 115, Academic Press Inc., Orlando, FL, 1984.

[13] Deuschel, J.-D.; Friz, P.; Jacquier, A.; Violante, S. Marginal density expansions for diffusions and stochastic volatility. February, 2012. Preprint.

[14] Duck, P. W.; Yang, C.; Newton, D. P.; Widdicks, M. Singular perturbation techniques applied to multiasset option pricing. *Math. Finance* **19** (2009), no. 3, 457–486. Available at: http://dx.doi.org/10.1111/j.1467-9965.2009.00373.x

[15] Evans, L. C.; Gariepy, R. F. *Measure theory and fine properties of functions*, Studies in Advanced Mathematics, CRC Press, Boca Raton, FL, 1992.

[16] Gatheral, J. *The Volatility Surface: A Practitioner's Guide*, Wiley Finance, John Wiley & Sons, 2006. Available at: http://books.google.de/books?id=9Y8rWE6mLOEC

[17] Gatheral, J.; Hsu, E. P.; Laurence, P.; Ouyang, C.; Wang, T.-H. Asymptotics of implied volatility in local volatility models. *Mathematical Finance* (2010), no–no. Available at: http://dx.doi.org/10.1111/j.1467-9965.2010.00472.x

[18] Gatheral, J.; Wang, T.-H. The heat kernel most likely path approximation. *International Journal of Theoretical and Applied Finance* **15** (2012), no. 1.

[19] Giles, M. B. Multilevel Monte Carlo path simulation. *Oper. Res.* **56** (2008), no. 3, 607–617. Available at: http://dx.doi.org/10.1287/opre.1070.0496

[20] Guyon, J.; Henry-Labordère, P. From local to implied volatilities. *Risk Magazine* (2011), no. May.

[21] Hagan, P.; Kumar, D.; Lesniewski, A.; Woodward, D. Managing smile risk. *Wilmott Magazine* (2002).

[22] Hagan, P.; Woodward, D. Equivalent Black volatilties. *Applied Mathematical Finance* **6** (2002), 147–157.

[23] Henry-Labordère, P. *Analysis, geometry, and modeling in finance*, Chapman & Hall/CRC Financial Mathematics Series, CRC Press, Boca Raton, FL, 2009.

[24] Hsu, P. Heat kernel on noncomplete manifolds. *Indiana Univ. Math. J.* **39** (1990), no. 2, 431–442. Available at: http://dx.doi.org/10.1512/iumj.1990.39.39023

[25] Ju, N. Pricing Asian and basket options via Taylor expansion. *Journal of Computational finance* (2002).

[26] Kusuoka, S. Approximation of expectation of diffusion processes based on Lie algebra and Malliavin calculus. pp. 69–83, Springer, Tokyo, 2004.

[27] Li, M.; Zhou, J.; Deng, S.-J. Multi-asset spread option pricing and hedging. *Quant. Finance* **10** (2010), no. 3, 305–324. Available at: http://dx.doi.org/10.1080/14697680802626323

[28] Linetsky, V.; Mendoza, R. Constant elasticity of variance (cev) diffusion model. in *Encyclopedia of Quantitative Finance*, edited by R. Cont, John Wiley & Sons, Ltd, 2010. Available at: http://dx.doi.org/10.1002/9780470061602.eqf08015

[29] Lyons, T.; Victoir, N. Cubature on Wiener space. *Proc. R. Soc. Lond. Ser. A Math. Phys. Eng. Sci.* **460** (2004), no. 2041, 169–198.

[30] Milevsky, M. A.; Posner, S. E. Asian options, the sum of lognormals, and the reciprocal gamma distribution. *Journal of Financial and Quantitative Analysis* **33** (1998), no. 03, 409–422. http://journals.cambridge.org/article_S0022109000001009. Available at: http://dx.doi.org/10.1017/S0022109000001009

[31] Milevsky, M. A.; Posner, S. E. A closed-form approximation for valuing basket options. *The Journal of Derivatives* (1998).

[32] Minakshisundaram, S. Eigenfunctions on Riemannian manifolds. *J. Indian Math. Soc. (N.S.)* **17** (1953), 159–165 (1954).

[33] Minakshisundaram, S.; Pleijel, Å. Some properties of the eigenfunctions of the Laplace-operator on Riemannian manifolds. *Canadian J. Math.* **1** (1949), 242–256.

[34] Molčanov, S. A. Diffusion processes, and Riemannian geometry. *Uspehi Mat. Nauk* **30** (1975), no. 1(181), 3–59.

[35] Ninomiya, S.; Victoir, N. Weak approximation of stochastic differential equations and application to derivative pricing. *Appl. Math. Finance* **15** (2008), no. 1-2, 107–121.

[36] Pellizzari, P. Efficient Monte Carlo pricing of European options using mean value control variates. *Decis. Econ. Finance* **24** (2001), no. 2, 107–126.

[37] Piterbarg, V. Markovian Projection Method for Volatility Calibration. *SSRN eLibrary* (2006).

[38] Reghai, A. The hybrid most likely path. *Risk* (2006).

[39] Schachermayer, W.; Teichmann, J. How close are the option pricing formulas of Bachelier and Black-Merton-Scholes? *Math. Finance* **18** (2008), no. 1, 155–170. Available at: http://dx.doi.org/10.1111/j.1467-9965.2007.00326.x

[40] Takahashi, A.; Shiraya, K. On multi-asset cross currency options. Working paper.

[41] Varadhan, R. S. Diffusion processes in a small time interval. *Comm. Pure Appl. Math.* **20** (1967), 659–685.

[42] Yosida, K. On the fundamental solution of the parabolic equation in a Riemannian space. *Osaka Math. J.* **5** (1953), 65–74.

Weierstrass Institute, Mohrenstr. 39, 10117 Berlin, Germany
E-mail address: christian.bayer@wias-berlin.de

Università di Roma 1 and Courant Institute of Mathematical Sciences, Piazzale Aldo Moro 2, I-00185 Roma, Italia
E-mail address: peter.laurence@gmail.com